# CALIBRATION BETWEEN FIBER-OPTIC PROBE BASED RAMAN SPECTROSCOPY SYSTEMS

By

Brittany Caldwell

Thesis

Submitted to the Faculty of the

Graduate School of Vanderbilt University

in partial fulfillment of the requirements

for the degree of

MASTER OF SCIENCE

In

Biomedical Engineering

December, 2011

Nashville, Tennessee

Approved:

Professor Anita Mahadevan-Jansen

Professor E. Duco Jansen

ACKNOWLEDGEMENTS

I would like to thank the Department of Defense for their financial support and funding of this research. Additionally, I would like to thank the Society of Women Engineer's for their financial support in awarding me a graduate fellowship. This work would not be possible without the help of my mentor, Dr. Anita Mahadevan-Jansen. I cannot thank you enough for your encouragement and energy towards making me a better researcher. I look forward to the next few years as I develop even further. Without the help of Dr. Quyen Nguyen, I would not have been able to understand Raman spectroscopy so well. For his patience and willingness to answer my numerous questions I will be forever grateful. I hope one day to share the breadth of your Raman spectroscopy knowledge.

I am grateful for my family who has always encouraged me to push towards my dreams, especially my Mom. You will never know how much I appreciate your love and support. Finally, I would like to thank Jed who has listened to my frustrations and still encourages me to achieve my dreams. I am so fortunate to have you in my life!

TABLE OF CONTENTS

LIST OF FIGURES

# CHAPTER I

# INTRODUCTION AND BACKGROUND

## Introduction

This project presents a new method to correct for day-to-day variations of Raman spectroscopy systems. The current gold standard to correct for wavelength dependent response of an optical system uses a NIST tungsten-lamp to measure changes in system throughput. However, the NIST lamp method does not account for source variation and does not appear to fully correct for the system response. An alternative method, presented in this work, has been developed based on using a plan reference standard, to correct for system variation from each element in a Raman spectroscopic system. Further, we seek to develop a method of rapidly correcting for day to day variation without the need for extensive experimentation.

Raman spectroscopy measures non-linear, optical interaction with molecules to determine the chemical fingerprint of a sample. When incident photons interact with the vibration modes of a molecule, the photons are scattered non-linearly. The energy difference of scattered photons is related to the energy of the specific bonds. Raman spectroscopic systems isolate and detect these scattered photons. The relative shift from the incident photon energy is measured in relative wavenumbers ($cm^{-1}$) and called the Raman shift. The count of photons detected at each Raman shift can then be plotted as a function of wavenumber to create a spectrum. A spectrum relates to the number

and type of bonds for the molecules within the measured material. Therefore, each different material measured will have a different spectrum. Samples of the exact composition should have the same Raman spectrum. Thus, the Raman spectrum provides a molecular/ chemical fingerprint that can be used to identify the specific vibrational modes of the molecules and therefore the specific bonds and identify of the molecule under study.

**History**

The Raman effect was first observed by Chandrasekhara Venkata Raman in 1928. His discovery earned him a Nobel prize in physics in 1930 (Gardiner and Graves 1989; Ferraro and Nakamoto 1994). Without the invention of the laser, early Raman spectroscopic systems consisted of a mercury lamp, filter, glass prism, and a photographic plate (Baranska, Labudzinska et al. 1987; Ferraro and Nakamoto 1994). A measured spectrum contained a high incident wavelength at the origin and symmetric Raman scattered bands at offset distances. Collection of these early spectra could take up to twenty four hours of exposure time for a single measurement(Gardiner and Graves 1989).

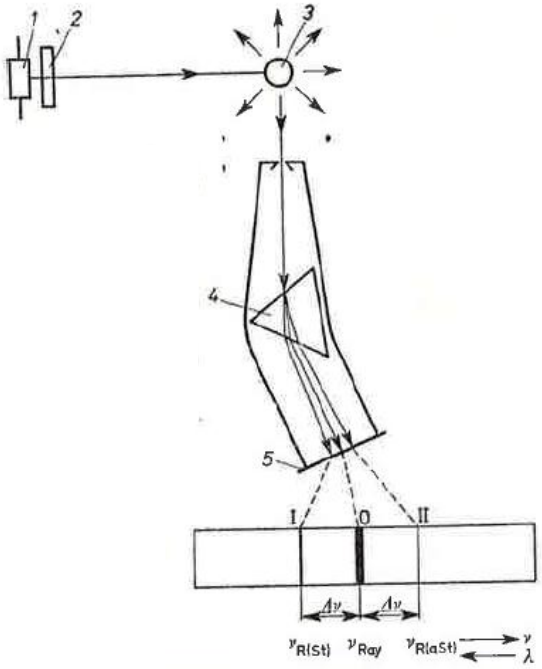


**Figure I.1** Early Raman spectroscopy system consisting of a mercury lamp (1), filter (2), sample being excited (3), prism to separate wavelengths (4), and a grating (5). To measure spectra with these instruments, long integration times were required. The data acquired, gave three bands for Rayleigh scattering, Raman Stokes scattering and anti-Raman stokes (Baranska, Labudzinska et al. 1987).

Modern Raman spectroscopy techniques started developing in the 1960s with the invention of continuous wave lasers. The procedure has revolutionized chemical analysis as measurements can be taken on microliter samples at different temperatures, pressures, and states of matter. Additionally, spectroscopy techniques including the Resonance Raman effect, stimulated Raman effect, hyper Raman effect, Raman gain spectroscopy, Raman induced Kerr effect spectroscopy, and the induced Raman effect have been discovered due to the development of Raman spectroscopy (Baranska, Labudzinska et al. 1987; Gardiner and Graves 1989).

## Theory

An incident photon interacting with a molecule can be scattered by inelastic or elastic scattering. Rayleigh scattering, otherwise known as elastic scattering, does not change the energy of the photon during the scattering process. Inelastic scattering based on the Raman effect occurs when energy is transferred from the molecule to the photon or from the photon to the molecule resulting in more or less energy of the scattered photon. The event of energy transferred from the molecule to the photon so that the photon has more energy is known as anti-Stokes scattering. Conversely, the transfer of energy from the photon to the molecule is called Stokes scattering. There are two theories, classical and quantum, to explain the Raman effect (Ferraro and Nakamoto 1994).

### Classical Theory

The classical theory to explain molecular interaction with the incident light assumes the molecule is vibrating at harmonic frequencies. A vibrating dipole is generated when an electromagnetic field fluctuating at a given frequency is incident on the molecule. The dipole moment produced, $\rho$ (coulomb-meter), is proportional to the electric field strength, E (volt/meter), as shown in equation 1.

$$\rho = \alpha E \qquad 1$$

Where α (Coulomb-meter$^2$/volt) represents the polarizability of a molecule. The electric field strength can be written to show its harmonic fluctuation in-terms of the intensity

amplitude, $E_o$ (volt/meter), wave frequency, $\nu_o$ (1/seconds), and time, t (seconds), as expressed in equation 2.

$$E = E_o \cos(2\pi t \nu_o) \quad (2)$$

Substituting this expression into equation 1 displays the fluctuations of the dipole moment induced by the electromagnetic wave (Ferraro and Nakamoto 1994).

$$\rho = \alpha E_o \cos(2\pi t \nu_o) \quad (3)$$

The polarizability of the molecule, which is a related to the mobility of the electrons and the shape and size of the molecule, can change during vibration. This change can be represented as shown in equation 4.

$$\alpha = \alpha_o + \left(\frac{\partial \alpha}{\partial Q_\nu}\right)_o Q_\nu \quad (4)$$

$Q_\nu$ represents the coordinate along the axis of vibration for the diatomic molecule, $\alpha_o$ represents the tensor at equilibrium position of the nuclei, and $\frac{d\alpha}{dQ_\nu}$ is the change of the polarizability in the course of the vibration. This coordinate value for a molecule vibrating at a specific frequency, $\nu_\nu$, can be written as $Q_\nu = Q_o cos(2\pi \nu_\nu t)$ where $Q_o$ represents the initial vibrational normal coordinate. Using this knowledge and equation 5, an equation for the incident dipole moment can be written.

$$\rho = \alpha_o E_o \cos(2\pi t \nu_o) + \left(\frac{\partial \alpha}{\partial Q_\nu}\right)_o E_o \cos(2\pi t \nu_o) Q_o \cos(2\pi t \nu_\nu) \quad (5)$$

Equation 5 can be rearranged using trigonometric identities to obtain equation 6 (Gilson and Hendra 1970).

$$\rho = \alpha_o E_o \cos(2\pi t v_o) + \frac{1}{2}\left(\frac{\partial \alpha}{\partial Q_v}\right)_o Q_o E_o \{\cos[2\pi t(v_o - v_v)] + \cos[2\pi t(v_o + v_v)]\} \quad 6$$

The first term in the equation represents Rayleigh scattering, where the frequency of vibrations is unchanged as displayed by the lack of frequency shift. The middle term represents Stokes scattering where the frequency is equal to the difference between the incident frequency and the vibrations of the molecule. The last term, representing anti-Stokes scattering, displays an increased in frequency of vibration by the summation of incident light and vibration of the molecule. (Ferraro and Nakamoto 1994). Additionally, this equation implies that for Raman scattering to occur, the polarizability of the molecule must change during excitation.

**Quantum Theory**

Absorption, stimulated emission, or scattering are the three outcomes from the interaction of an incident photon with a molecule. Absorption occurs when the energy of the photon corresponds to the difference between two energy levels of the molecule, in which case the photon energy is transferred to the molecule (Freeman 1974). Stimulated emission occurs when the incident photon provokes the emission of photons from the excited molecule. The energy emitted corresponds to the energy difference between the excited states and the ground state. The last phenomena, scattering, occurs when a photon is excited to a virtual state and then falls back to a lower energy state immediately (within $10^{-14}$ seconds). The photon energy does not correspond to a difference between two energy levels of a molecule during scattering. As the process is due to two photons, scattering cannot be separated into two distinct interactions of

absorption and emission. Elastic scattering, or no change in energy of the incident photon, is known as Rayleigh scattering. If there is a change in energy, two consequences can happen. An increase in photon energy, and therefore decrease in molecule energy can occur, and is known as anti-Stokes scattering. Conversely Stokes scattering happens if there is a decrease in photon energy and increase in molecule energy (Ferraro and Nakamoto 1994).

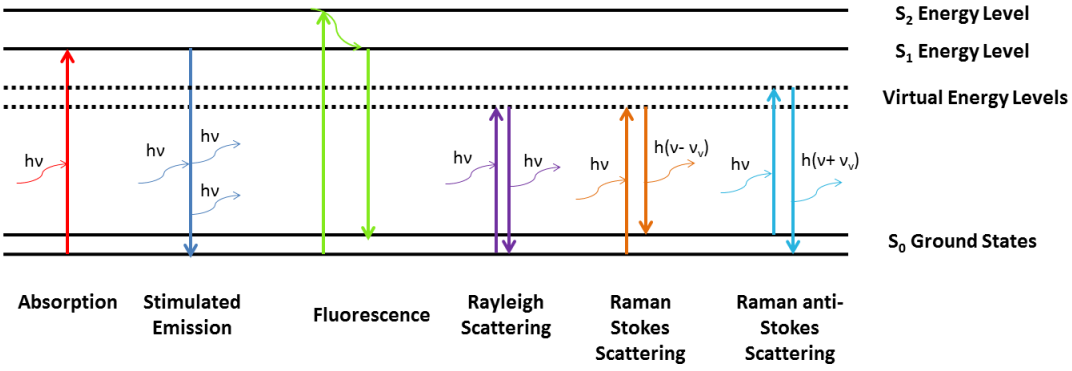


**Figure I.2** Jablonski diagram displaying interactions of molecules due to incident light. During absorption, the incident photon is absorbed. For stimulated emission, one photon is emitted after interaction with the incident photon. In fluorescence, light of a specific wavelength is absorbed and then a fluorescent light of a longer wavelength is emitted. Rayleigh scattering is the movement to a virtual energy state and back down to the original energy, indicating elastic scattering. Stokes scattering is the movement to a virtual energy state and back down to a level higher than initially, indicating a loss of photon energy and gain of molecule energy. Anti-Stokes Raman scattering is the loss of molecule energy and gain of photon energy as the final energy state is lower than the initial.

A Jablonski diagram can be used to describe the photon and molecule interaction as shown in Figure I.2. Rayleigh scattering, or elastic scattering is shown by the identical initial and final energies of the photon and molecule. The changes in photon and molecule energy in Raman scattering for both Stokes and anti-Stokes is also presented. At standard temperatures, most molecules are in the ground vibrational

state and therefore Stokes Raman scattering is more accessible and thus more common than Anti-Stokes Raman (Ferraro and Nakamoto 1994).

## Applications of Raman Spectroscopy

The applications of Raman spectroscopy have greatly increased since the Raman effect was discovered. One early Raman experiment performed in 1962 by Porto, Wood, and Stoicheff measured the spectra from carbon tetrachloride and benzene with a pulsed ruby laser. In their experiments, the sample was placed in a glass cell and through the use of a lens, the scattered light was collected. This early system displayed the need for a continuous wave laser source (Porto and Wood 1962; Gilson and Hendra 1970). To adapt to this need, Porto and Kogelnik placed chemicals within a Helium-neon laser cavity. An exposure time of 1 hour was required to obtain a spectrum, a decrease from the early 24 hour experiments done using sunlight and mercury lamps (Kogelnick and Porto 1963). In 1964, the company Perkin-Elmer developed a Raman laser machine. This device, the first of its kind, is often considered the “grandfather” of Raman instruments. This system used a Helium-neon laser to excite samples with only 6mW of power. Even with a low power, it was able to measure spectra from solids and liquids, displaying the diversity of Raman for sampling in a variety of states (Gilson and Hendra 1970). A year later, another early Raman system, the Cary 81 spectrometer was invented. It used a Helium-neon laser with 65mW of power to illuminate samples. The higher power not only improved the signal of a Raman spectrum, but also allowed liquid samples as small as 0.02 ml to be measured (Gilson and Hendra 1970; Adar, Delhaye et

al. 2003). These early Raman spectroscopic systems led the way to increased research and system development. As Raman instruments improved in capability, new techniques to apply Raman spectroscopy developed.

Macrospectroscopic systems are designed for sampling large volumes without strong focusing. These systems contain all the optical components needed to take a measurement within itself. Macroscopic systems have been developed for many individualized techniques within different industries. For example, Raman spectroscopy is often used in the pharmaceutical industry to analyze the composition of tablets or liquid medicines (Matousek and Parker 2006; Matousek and Parker 2007; Eliasson, Macleod et al. 2008; Aina, Hargreaves et al. 2010; Matousek, Thorley et al. 2011). Crystalline structure and orientation can also be studied by Raman spectra. The treatment of a gemstone to increase its clarity or color is a problem within the geotechnical industry. Raman spectroscopy has been applied to determine the presence of artificial additives without injuring the stone (Yoshikawa, Katagiri et al. 1989; Chalain, Fritsch et al. 2000). Forensic and security agencies also use Raman spectroscopy as it provides a technique that is able to determine a substance without compromising a sample (Claybourn and Ansell 2000; Miller and Bartick 2001; Izake 2010).

In the eighties, Raman spectroscopy was used to study tissues and cells. These early studies gave the community bio-chemical information on DNA and protein that had not been known before (Parker 1986; Yada, Jackman et al. 1988; Kennard and Hunter 1989; Steitz 1990). As detection capabilities and diode laser technology improved, detection of the weak biological Raman signal from tissues for disease

detection became possible. From the nineties to present, research has progressed to move towards in vivo applications of Raman spectroscopy (Mahadevan-Jansen and Richards-Kortum 1996; Vo-Dinh, Allain et al. 2002; Keller, Kanter et al. 2006; Keller, Kanter et al. 2008; Lieber, Majumder et al. 2008). For diagnostic applications, weak biological signals are obtained from a patient in a clinical setting. These systems must be moveable, adaptable to different environments, and have the proper resolution to accurately measure the biological signal. Currently, manufactured systems for this application are limited. Therefore, many biomedical researchers assemble systems from individual components which have the specific properties needed for an application.

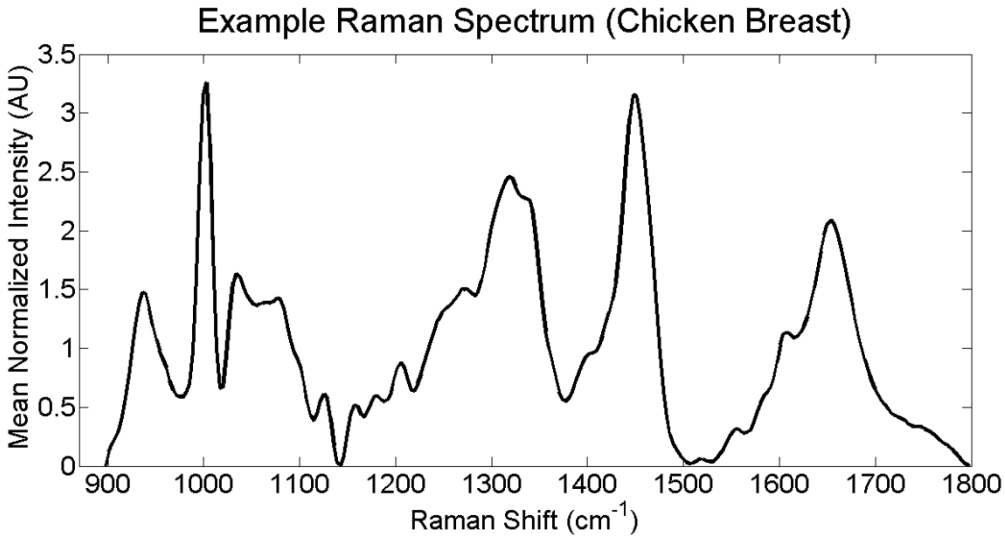


**Figure I.3 An example Raman spectrum of chicken breast after wavenumber calibration and fluorescence background subtraction. The spectrum shows wide peaks that are typically seen in biological spectra due to the varying type and organization of different molecules. Since the Raman spectrum is due to the type and orientation of molecules and their bonds, each material will have a unique spectrum. Comparison of these spectra allows researchers to classify samples.**

## Instrumentation

A Raman system for biomedical applications typically consists of four major components including a laser, spectrograph, detector, and a sample delivery and collection method. The Raman signal from biological tissue is weak, thus for these applications a system must be capable of measuring small molecular interactions. Biomedical studies often require systems to be portable between measurement locations. When assembling systems for this application, the size and weight of each component can be a strong factor in their selection. These constraints often lead to the purchasing of individual constituents through different companies to maximize a system's potential. The number of manufacturers and models within each company

creates a large selection of options to construct a system. Furthermore, there is a lack of specific standards for each individual component. Thus, there are an endless number of different systems that can be built. This complexity causes a lack of uniformity within biomedical Raman systems, leading to differences when comparing spectra from different instruments.

**Source**

Sources of illumination for Raman measurements have greatly improved from the original use of filtered sunlight. Sunlight and mercury lamps to illuminate samples required long exposure times and therefore limited the use and applications of Raman spectroscopy. (Baranska, Labudzinska et al. 1987; Gardiner and Graves 1989). However, with the invention of the laser, measurement times and minimum sample sizes were decreased. Lasers present an incident beam that is monochromatic, coherent, polarized, and has a set beam direction and width with low divergence (Baranska, Labudzinska et al. 1987). The ability to focus the incident light decreased the interrogation volume and increased the excitation intensity, thus resulting in a stronger Raman signal from the reduced volume (Freeman 1974). Lasers used in Raman studies may be pulsed or continuous wave. Pulsed lasers are used for high power studies, including nonlinear methods like surfaced enhanced Raman spectroscopy (SERS) (Gardiner and Graves 1989). Continuous wave lasers, the more common source for Raman measurements, provide a constant excitation source that can illuminate a sample at low powers. Common laser types for Raman measurements include Argon,

Krypton, Titanium-Sapphire, Helium-neon (He-Ne), yttrium aluminium garnet (YAG), and diode(Gilson and Hendra 1970; Stroemmen and Nakamoto 1984; Baranska, Labudzinska et al. 1987; Gardiner and Graves 1989; Hanlon, Manoharan et al. 2000; Vo-Dinh 2003). For systems where portability is needed, diode lasers are often used due to their compact size (Vo-Dinh 2003). Depending on the sample, a specific wavelength should be chosen to excite a sample. This value for biological tissues is typically 785 nm to ensure that the laser does not cause ablation to the sample.

**Spectrograph**

A spectrograph is used to spatially disperse as a function of wavelengths so that the detector can then record photon counts at different Raman shifts. Spectrographs are usually comprised of gratings and at least one mono or polychromator. The mono or polychromator(s) spatially selects and transmits a bandwidth of light from the collected spectrum using a diffraction grating (Baranska, Labudzinska et al. 1987; Stencel 1990; Hanlon, Manoharan et al. 2000). Raman scattering is a very weak event overshadowed by Rayleigh scattering which is $10^7$ to $10^8$ times stronger. Thus, the spectrometer must be capable of distinguishing the spectral region containing Raman shifted photons from the un-shifted spectral region. Furthermore, the spectrometer must have a high enough spectral resolution to distinguish the numerous individual Raman shifted peaks. In general, a spectral resolution of at least 8 $cm^{-1}$ is needed to resolve the Raman signal for biomedical applications (Baranska, Labudzinska et al. 1987; Vo-Dinh 2003). Multiple gratings are often used to increase the resolving power of a spectrograph and further

filter Rayleigh scattering which causes background noise (Baranska, Labudzinska et al. 1987; Stencel 1990). Commercially available spectrographs often contain double or triple monochromators. The multiple monochromators limit Rayleigh light, as well as light scattered off the gratings within the monochromator cavity from reaching the detector (Freeman 1974; Ferraro and Nakamoto 1994). These spectrographs also have additional filters and optics to reject unwanted signal and direct the light towards the monochromator. For fiber-optic probe based systems, spectrographs can be bought which are optimized for the transmission of signal from the fiber-optic probes (Stone, Stavroulaki et al. 2000; Utzinger, Heintzelman et al. 2001; Vo-Dinh 2003). Kaiser Optics and Princeton Instruments are two examples of companies that provide spectrographs which are designed for fiber-optic probe based systems. These systems are small, durable, and have adjustable probe connections to allow easy probe attachment (Vo-Dinh 2003).

**Detectors**

A detector is used to measure the intensity of photons at the specified wavelength after the collected light has been separated by a spectrometer. Traditionally detectors were photomultiplier tubes or photodiodes. However, charged coupled devices (CCD) have become popular detectors in current Raman spectroscopy studies (Gardiner and Graves 1989; Ferraro and Nakamoto 1994). The quality of a detector is determined by the background noise, sensitivity, and frequency range. Photomultipliers have high sensitivity and low background noise, however they do not have a linear

response over a full range of wavelengths and can be slow when recording measurements.(Baranska, Labudzinska et al. 1987; Ferraro and Nakamoto 1994). Photodiodes are often arranged as diode arrays to cover a range of wavelengths. These arrays are typically 1,024 diodes long so that each diode detects one wavelength of the spectrum (Gardiner and Graves 1989; Ferraro and Nakamoto 1994). A disadvantage of photodiodes is their strong sensitivity to high photon counts. Thus, extended exposure at high intensities, such as Raman peaks, deteriorates photodiodes within an array non-uniformly, resulting in decreased peak height over time (Baranska, Labudzinska et al. 1987; Gardiner and Graves 1989; Stencel 1990; Ferraro and Nakamoto 1994). When choosing between a photomultiplier or photodiode detector, the type of work and necessary limitations determine which component will be most efficient.

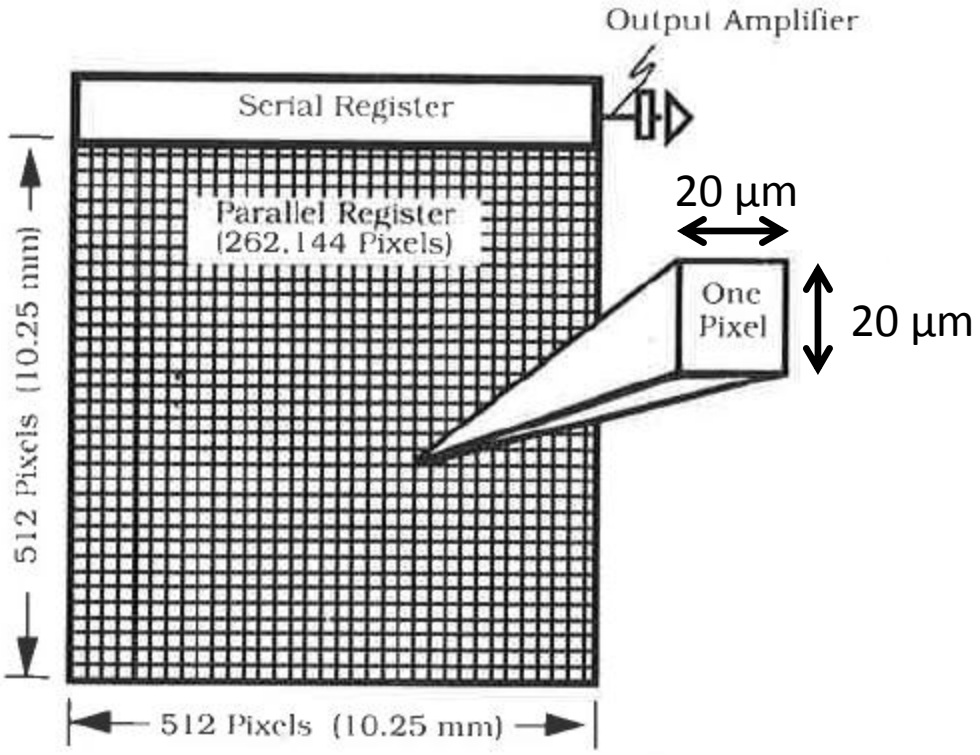


**Figure I.4** A modern CCD comprised of 262,144 individual pixels. Each pixel serves as an individual counter of photon collection. Horizontal location can be calibrated to relate to specific wavelengths while the vertical structure allows input from multiple fibers stacked vertically. CCDs have high quantum efficiency and relatively low noise to allow the measure of weak Raman signals (Ferraro and Nakamoto 1994).

The third type of popular detector for Raman spectroscopy measurements is a charge-coupled device (CCD). CCDs are photosensitive pixels arranged into a square array, typically called a focal plane array (FPA). Horizontal location within the FPA relates to wavelengths, determined by calibration measurements. The vertical axis can be used for multiple stacked fiber inputs from a fiber-optic probe so that a higher signal can be recorded. CCDs can be made of different materials including silicon, indium gallium arsenide, and germanium to detect at different ranges in the wavelength spectrum. For example, silicon-based detectors are often used to detect at wavelengths

of 300-1100nm(Vo-Dinh 2003). Back-illuminated, deep depletion CCDs are optimal for use in near-infrared biomedical applications as they can detect low amounts of light. An advantage of using a CCD is the low readout noise and high quantum efficiency and sensitivity compared to other detectors (Ferraro and Nakamoto 1994; Vo-Dinh 2003). Readout noise is due to the electronics creating a signal which in turn becomes digitized with the pixel charge. This creates a false identification of photons and can alter the accuracy of peak heights. Quantum efficiency of a CCD is measured as the percentage of photons which strike a photo-reactive surface and result an electron-hole pair. This number relates to the device's sensitivity to light, thus high quantum efficiency indicates the ability of a CCD to accurately detect photons. Most fiber-optic probe based Raman spectroscopic systems used today for biomedical applications use a CCD as a detector due to their low readout noise and high quantum efficiencies which help when measuring weak biological samples (Gardiner and Graves 1989; Hanlon, Manoharan et al. 2000; Vo-Dinh 2003).

**Sample Delivery and Collection**

In bulk systems, a sample can be placed within a compartment of the system to be measured. However, for *in vivo* biomedical applications, a patient's tissue cannot be placed into a compartment. Fiber-optic probes have been developed to allow measurements away from the system. Probes are built to deliver the excitation light to the tissue and to collect scattered light to the system after tissue interaction (Stencel 1990; Vo-Dinh 2003). The type of probe and set up depends upon the design and

purpose of the probe. Silica optical fibers are commonly used for biomedical applications. However, their Raman signal, proportional to the fiber length, will be added to the collected spectrum (Myrick, Angel et al. 1990; Mahadevan-Jansen and Richards-Kortum 1996). To correct for this unwanted signal, a band-pass filter can be placed on the edge of the excitation fiber so that only light of the source wavelength excites the sample. On the collection fibers a long-pass or notch filter can prevent excitation and elastically scattered light from being detected as Raman signal (Angel and Myrick 1990; Myrick, Angel et al. 1990). Orientation of detection fibers is dependent on the sample; however the use of multiple detection fibers is often preferred to increase the detected signal (McLachlan, Jewett et al. 1986; Cothren, Richards-Kortum et al. 1990; Schomacker, Frisoli et al. 1992; Ramanujam, Mitchell et al. 1996). A common design is a single excitation fiber surrounded by multiple detection fibers. This design is used in probes designed by EMVision described in this study where seven collection fibers surround one excitation fiber (Marple 2009). Probe selection is extremely important as it will greatly affect the signal and delivery capabilities.

## Current Correction Methods

Each Raman spectroscopic system has a wavelength dependent response. This overall system response can be affected by any disturbance in the setup, including jarring or realignment. Changes in the system response will cause differences spectra from a sample. Each time measurements are taken, a calibration must be done to

correct for any change in the system due to day-to-day variation. Two previous methods to correct for adjustments in response are described below.

**NIST Tungsten lamp**

To correct for changes in system response, the National Institute of Standards and Technology (NIST) developed a method which uses a tungsten lamp as a calibration standard, shown in Figure I.4 (Lackowicz 1999; DeRose, Early et al. 2007; DeRose, Early et al. 2008). NIST provides a polynomial which represents the throughput of a Raman system collecting the light. This curve, which closely resembles a line, is used to compare spectra of the lamp to. A measurement of a system's throughput of the lamp will change depending on the instruments alignment. To obtain correction factors, a measured throughput curve is divided into the polynomial given by NIST. As the system response changes, the correction factors will change to reflect the throughput changes.

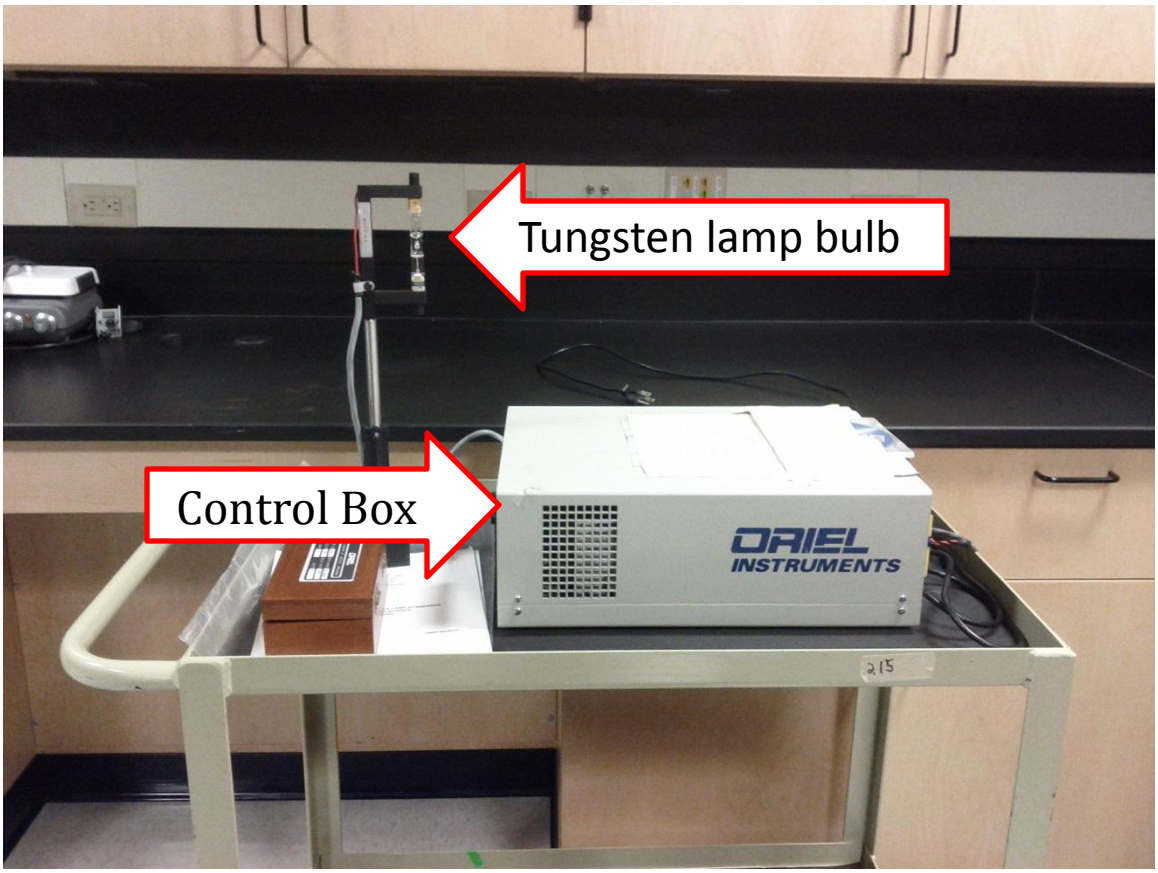


**Figure I.5** NIST tungsten lamp system. Measurement of lamp by a Raman system measures the overall throughput of the system. This spectrum can then be compared to the ideal spectrum to obtain correction factors to correct for changes in system response. Correction factors gained using this lamp do not account for the source component.

Using the NIST tungsten lamp provides the gold standard method to correct for system throughput changes. Since the technique considers only the throughput response of the system, it does not correct for adjustments in system response due to the source. The development of a method to correct for both, the detection and source components of a system, is necessary to completely correct for day-to-day system variation. A complication with the use of the tungsten lamp as a calibration standard for fiber-optic probe based systems is the measured throughput dependence on filters at

the tip of each probe. The filters have an angular dependence which causes the lamp spectrum to change depending on the orientation of the probe. To decrease this contingency, a probe must be moved randomly during a measurement so that a non-angular dependent spectrum is measured. This method to adjust for the filtered response is contingent on the individual taking measurements and the randomness or lack thereof in their ability to rotate the probe. Last, this standard is impractical to use within a clinical setting due to space and safety. When obtaining a system's throughput, the system must be far enough away from the lamp to avoid saturation. Additionally, all individuals with contact to the light must wear eye protection. In a clinical room, it is difficult to achieve both of these constraints. To allow the use of the lamp as a calibration standard, Raman spectroscopic systems are currently moved to a non-clinical location to obtain a lamp spectrum. Movement will likely cause components to be jarred slightly, meaning the system response corrected for will not be the same as when measurements were taken. This causes the tungsten lamp calibration to be inaccurate and not beneficial in clinical settings.

**NIST Glass Standard**

In response to the difficulties of using the NIST tungsten lamp, a glass was developed by NIST to be used as a standard to correct for system response (DeRose, Smith et al. 2008; DeRose, Smith et al. 2009; Locascio and Watters 2010). To measure changes due to the system response, a measurement is taken on the glass. By measuring an object instead of the throughput of a lamp, changes due to the source can

be calibrated for. The correction factors for this material are obtained by dividing the measured spectrum into a given polynomial, similar to the tungsten lamp method. The glass standard allows a method to calibrate for day-to day system response changes in a clinical setting. However, this standard is no longer on the market due to a lack of spatial and temporal stability. Without spectral satiability, the glass spectrum will not properly measure changes in system response (Krishnamoorthi, Gasparino et al. 2010).

## Motivation and Significance

Currently, there is no method which will reliably correct for day-to-day variation in fiber-optic probe based Raman spectroscopic systems. Each time measurements are taken, systems must be aligned to ensure high throughput for maximum Raman signal, causing instrument changes. Mobility of clinical systems increases the day-to-day variation that must be corrected for. Without a method to calibrate for changes in system variation, accurate classification of diseased and non-diseased spectra cannot occur. Consequences from inaccurate classification for biomedical studies can be high, stressing the need to have a method to correct for system variation. Increased accuracy in the ability to determine minute chemical differences from diseased and non-diseased tissue samples will result with this correction.

## Hypothesis and Objectives

The goal of this study is to determine a new method to correct for changes in the instrument response for Raman spectroscopic systems. A standard to use in a

calibration technique must fit the constraints needed for use in a clinical setting. Additionally, a method to perform the calibration must be developed. The last aim of the study is to validate the new method and evaluate its performance in correcting for changes in system response.

The Vanderbilt Biomedical Photonics Laboratory has previously tested the spectrum from a piece of glass obtained from an unknown wine bottle. The Raman spectrum from this bottle was shown to be spatially and temporally stable and its spectrum to have an overall fluorescence throughput curve with low Raman signal (Krishnamoorthi, Gasparino et al. 2010). By correcting the glass spectrum with the NIST tungsten lamp, a corrected glass spectrum was created. This corrected glass spectrum was used as a standard curve to compare future measurements to. Initial studies showed that the glass could be used as a standard for calibrating to correct for day-to-day system variation.

The first part of this study will be to test different types of glass, including filters and wine bottles, to determine if any provide the same or a similar spectrum to that of the unknown glass. The spectrum of the unknown glass, a fluorescent curve with no Raman, has the properties which are ideal for a standard to correct for changes in system response. Glasses which have this spectrum will also be tested for spatial and temporal variability. Last, a correction method will be developed and implemented to test the feasibility and accuracy of correcting for changes in system response by a measured glass spectrum. To determine the breadth of the correction technique, it will

be tested for system response changes due to different probes and to different spectrograph and CCD combinations.

This thesis will focus on providing and implementing a new correction method for changes in system response of fiber-optic probe based Raman spectroscopic systems. The results are expected to display the ability of a piece of glass to be used as a calibration standard for system changes. Demonstrating the ability to correct for day-to-day variation for Raman spectroscopic systems in clinical situations will provide researchers a new, simple and inexpensive method to implement correction.

## Bibliography


Adar, F., M. Delhaye, et al. (2003). Evolution of Instrumentation for Detection of the Raman Effect as Driven by AVailable Technologies and by Developing Applications. Pittcon.

Aina, A., M. D. Hargreaves, et al. (2010). "Transmission Raman spectroscopy as a tool for quantifying polymorphic content of pharmaceutical formulations." Analyst **135**(9): 2328-2333.

Angel, S. M. and M. L. Myrick (1990). "Wavelength Selection for Fiber Optic Raman-Spectroscopy .1." Applied Optics **29**(9): 1350-1352.

Baranska, H., A. Labudzinska, et al., Eds. (1987). Laser Raman Spectroscopy. New York, Polish Scientific Publishers.

Chalain, J. P., E. Fritsch, et al. (2000). "Identification of GE POL diamonds: a second step." Journal of Gemmology **27**(2): 73-78.

Claybourn, M. and M. Ansell (2000). "Using Raman Spectroscopy to solve crime: inks, questioned documents and fraud." Science & Justice **40**(4): 261-271.

Cothren, R. M., R. Richards-Kortum, et al. (1990). "Gastrointestinal Tissue Diagnosis by Laser-Induced Fluorescence Spectroscopy at Endoscopy." Gastrointestinal Endoscopy **36**(2): 105-111.

DeRose, P. C., E. A. Early, et al. (2007). "Qualification of a fluorescence spectrometer for measuring true fluorescence spectra." Review of Scientific Instruments **78**(3).

DeRose, P. C., E. A. Early, et al. (2008). Measuring and Certifying True Fluorescence Spectra with a Qualified Fluorescence Spectrometer. 5th Oxford Conference on Spectrometer, Crown, UK.

DeRose, P. C., M. V. Smith, et al. (2008). "Characterizaton of Standard Reference Materials 2941, Uranyl-Ion-Doped Glass, Spectral Correction Standard for Fluorescence." Journal of Luminescence **128**: 257-266.

DeRose, P. C., M. V. Smith, et al. (2009). "Characterization of Standard Reference Materials 2940, MN-Ion-Doped Glass, Spectral Correction Standard for Fluorescence." Journal of Luminescence **129**: 349-355.

Eliasson, C., N. A. Macleod, et al. (2008). "Non-invasive quantitative assessment of the content of pharmaceutical capsules using transmission Raman spectroscopy." Journal of Pharmaceutical and Biomedical Analysis **47**(2): 221-229.

Ferraro, J. R. and K. Nakamoto (1994). Introductory Raman Spectroscopy. New York, Academic Press, Inc.

Freeman, S. K. (1974). Applications of Laser Raman Spectroscopy. New York, John Wiley & Sons.

Gardiner, D. J. and P. R. Graves, Eds. (1989). Practical Raman Spectroscopy. New York, Springer-Verlag Berlin Heidelberg.

Gilson, T. R. and P. J. Hendra (1970). Laser Raman Spectroscopy. New York, Wiley-Interscience.

Hanlon, E. B., R. Manoharan, et al. (2000). "Prospects for in vivo Raman spectroscopy." Physics in Medicine and Biology **45**(2): R1-R59.

Izake, E. L. (2010). "Forensic and homeland security applications of modern portable Raman spectroscopy." Forensic Science International **202**(1-3): 1-8.

Keller, M. D., E. M. Kanter, et al. (2008). "Detecting temporal and spatial effects of epithelial cancers with Raman spectroscopy." Disease Markers **25**(6): 323-337.

Keller, M. D., E. M. Kanter, et al. (2006). "Raman spectroscopy for cancer diagnosis." Spectroscopy **21**(11): 33-41.

Kennard, O. and W. N. Hunter (1989). "Oligonucleotide Structure - a Decade of Results from Single-Crystal X-Ray-Diffraction Studies." Quarterly Reviews of Biophysics **22**(3): 327-379.

Kogelnick, H. and S. P. S. Porto (1963). "Continuous Helium-Neon Red Laser as a Raman Source." Journal of The Optical Society of America **53**(12): 1446-1447.

Krishnamoorthi, H., N. Gasparino, et al. (2010). Calibration of Raman Systems for Biomedical and Clinical Applications. SPIE Photonics West, San Francisco, CA.

Lackowicz, J. R. (1999). Principles of Fluorescence Spectroscopy. New York, Kluwer Academic/Plenum Publishers.

Lieber, C. A., S. K. Majumder, et al. (2008). "Raman microspectroscopy for skin cancer detection in vitro." Journal of Biomedical Optics **13**(2).

Locascio, L. and R. Watters (2010). Standard Reference Material 2241. Relative Intensity Correction Standard for Raman Spectroscopy: 785 nm Excitation. Gaithersburg, MD, National Institute of Standards and Technology; Department of Commerce, United States of America**:** 6.

Mahadevan-Jansen, A. and R. Richards-Kortum (1996). "Raman spectroscopy for the detection of cancers and precancers." Journal of Biomedical Optics **1**(31).

Mahadevan-Jansen, A. and R. Richards-Kortum (1996). "Raman Spectrscopy for the Detection of Cancers and Precancers." Journal of Biomedical Optics **1**(1): 31-70.

Marple, E. (2009). High Collection Efficiency Fiber Optic Probes. U. P. Office. United States, Prescient Medical, Inc.

Matousek, P. and A. W. Parker (2006). "Bulk Raman analysis of pharmaceutical tablets." Applied Spectroscopy **60**(12): 1353-1357.

Matousek, P. and A. W. Parker (2007). "Non-invasive probing of pharmaceutical capsules using transmission Raman spectroscopy." Journal of Raman Spectroscopy **38**(5): 563-567.

Matousek, P., F. Thorley, et al. (2011). "Emerging Raman Techniques for Rapid Noninvasive Characterization of Pharmaceutical Samples and Containers." Spectroscopy **26**(3): 44-51.

McLachlan, R., G. Jewett, et al. (1986). Fiber-Optic Probe for Sensitive Raman Analysis. U. S. P. Office. United States, The Dow Chemical Company.

Miller, J. V. and E. G. Bartick (2001). "Forensic analysis of single fibers by Raman spectroscopy." Applied Spectroscopy **55**(12): 1729-1732.

Myrick, M. L., S. M. Angel, et al. (1990). "Comparison of Some Fiber Optic Configurations for Measurement of Luminescence and Raman-Scattering." Applied Optics **29**(9): 1333-1344.

Parker, F. S. (1986). "Biochemical Applications of Fourier-Transform Infrared-Spectroscopy." Canadian Journal of Spectroscopy **31**(1): 1-6.

Porto, S. P. S. and D. L. Wood (1962). "Ruby Optical Maser as a Raman Source." Journal of Optical Scoiety of Americal **52**(3): 251-252.

Ramanujam, N., M. F. Mitchell, et al. (1996). "Spectroscopic diagnosis of cervical intraepithelial neoplasia (CIN) in vivo using laser-induced fluorescence spectra at multiple excitation wavelengths." Lasers in Surgery and Medicine **19**(1): 63-74.

Schomacker, K. T., J. K. Frisoli, et al. (1992). "Ultraviolet Laser-Induced Fluorescence of Colonic Tissue - Basic Biology and Diagnostic Potential." Lasers in Surgery and Medicine **12**(1): 63-78.

Steitz, T. A. (1990). "Structural Studies of Protein Nucleic-Acid Interaction - the Sources of Sequence-Specific Binding." Quarterly Reviews of Biophysics **23**(3): 205-&.

Stencel, J. (1990). Raman Spectroscopy for Catalysis. New York, Van Nostrand Reinhold.

Stone, N., P. Stavroulaki, et al. (2000). "Raman spectroscopy for early detection of laryngeal malignancy: Preliminary results." Laryngoscope **110**(10): 1756-1763.

Stroemmen, D. P. and K. Nakamoto (1984). Laboratory Raman Spectroscopy. New York, Wiley-Interscience.

Utzinger, U., D. L. Heintzelman, et al. (2001). "Near-infrared Raman spectroscopy for in vivo detection of cervical precancers." Applied Spectroscopy **55**(8): 955-959.

Vo-Dinh, T., Ed. (2003). Biomedical Photonics Handbook. Raman Spectroscopy: From Benchtop to Bedside. Washington, DC, CRC Press.

Vo-Dinh, T., L. R. Allain, et al. (2002). "Cancer gene detection using surface-enhanced Raman scattering (SERS)." Journal of Raman Spectroscopy **33**(7): 511-516.

Yada, R. Y., R. L. Jackman, et al. (1988). "Secondary Structure Prediction and Determination of Proteins - a Review." International Journal of Peptide and Protein Research **31**(1): 98-108.

Yoshikawa, M., G. Katagiri, et al. (1989). "Characterization of Crystalline Quality of Diamond Films by Raman-Spectroscopy." Applied Physics Letters **55**(25): 2608-2610.

# CHAPTER II

# CALIBRATION OF RAMAN SPECTROSCOPY SYSTEMS

## Introduction

Raman spectroscopy provides a chemical fingerprint for a measured sample. The peaks within a spectrum correlate to the chemical bonds, environment, and organization between molecules. Thus, minute chemical differences between samples can be detected by changes in a spectrum. Adjustments in system response to do the instrument jolting or re-alignment will alter the throughput and therefore change the spectrum. The sensitivity of detection is limited to correcting for changes in system response due to day-to-day variation.

Fiber-optic probe based systems are often assembled from individual components as there are very few complete systems on the commercial market. Thus, each system can be comprised of devices from a variety of manufacturers and different models within a single manufacturer. The lack of similarity between systems causes the inability to compare measurements taken from different systems as the shape each systems wavelength dependent response curves can differ. However, even within a single system, measurements can be difficult to compare. If a component is jarred or a fiber-optic probe removed and replaced, the system response will be changed. Different instrument throughputs cause changes within the spectra, making data obtained before and after the system is altered incomparable.

Fiber-optic probe based Raman spectroscopic systems are often used for biomedical applications, for example, disease detection and tissue characterization. Recently, these systems have been applied for disease diagnosis within a clinical setting (Mahadevan-Jansen and Richards-Kortum 1996; Vo-Dinh, Allain et al. 2002; Keller, Kanter et al. 2006; Keller, Kanter et al. 2008; Lieber, Majumder et al. 2008). In these studies, measurements are often taken on patients within a clinical examination room or operating room. To obtain measurements in these locations, a system is transported between a laboratory and clinical setting regularly, causing shifting of components. Additionally, fiber optic probes are continuously removed between measurements so that the probe can be protected during movement. Removal and replacement of a probe has been shown in previous studies to be a large source of changes in the response of a system (Whisenant and Gasparino 2007).The inaccurate diagnosis of a clinical disease can have major consequences for the patient. Therefore, it is important to be able to correct for changes in system response.

## Current Method

The National Institute for Standards and Technology (NIST) addressed the need for a method of calibration to correct for changes in system response by the use of a tungsten calibrated lamp (Frost and McCreery 1998; Lackowicz 1999; DeRose, Early et al. 2007; DeRose, Early et al. 2008). This lamp, commonly known as “white light”, serves as the primary standard to remove the effect of wavelength dependent responses from measurements. A polynomial curve given by NIST, which is close to a straight line,

represents the throughput of a system collecting the lamp light. This curve can be viewed in Figure II.1a. To obtain correction factors, a system's throughput of the lamp light is collected. An example of the throughput curve measured from a fiber-optic probe based system is displayed in Figure II.1c. Each time a system's alignment is changed, the spectrum of the lamp will be altered. Correction factors are achieved by dividing the system's measured lamp spectrum into the polynomial given from NIST, as seen in Figure II.1e. Applying these correction factors adjusts for the changes in system response to allow comparison between spectra. The modification to the spectra can be observed in Figure II.1g where the gray line represents the spectrum before the application of the correction factors. The black line indicates the spectrum after the wavelength dependent response has been removed.

**Advantages and Disadvantages**

This method is the gold standard to calibrate for changes in system response. However, this technique only calibrates for the detection components of a system and not the source. The delivery of the excitation light can also cause changes within a system response. An additional complication is the difficulty of taking measurements in a medical setting. Spectra of the lamp must be taken at a distance far enough away to avoid saturation. Moreover, eye protection must be worn by all individuals in the room when a measurement is taken. These two constraints are difficult to meet within an examination or operating room. Furthermore, the shape of a lamp spectrum is dependent on the filters placed at the tip of a probe. These filters cause an angular

dependence on the transmitted spectrum. To account for this dependence, an individual must rotate the probe randomly so that the effect of the filters can be diminished. These complications make measurements of the lamp difficult in biomedical experiments. To account for these, NIST created a glass standard (Choquette 2005; Choquette, Etz et al. 2007; DeRose, Smith et al. 2008; DeRose, Smith et al. 2009; Locascio and Watters 2010). This standard was meant to provide a calibration spectrum which could account for day-to-day variation. However, the standard lacked spatial and temporal stability.

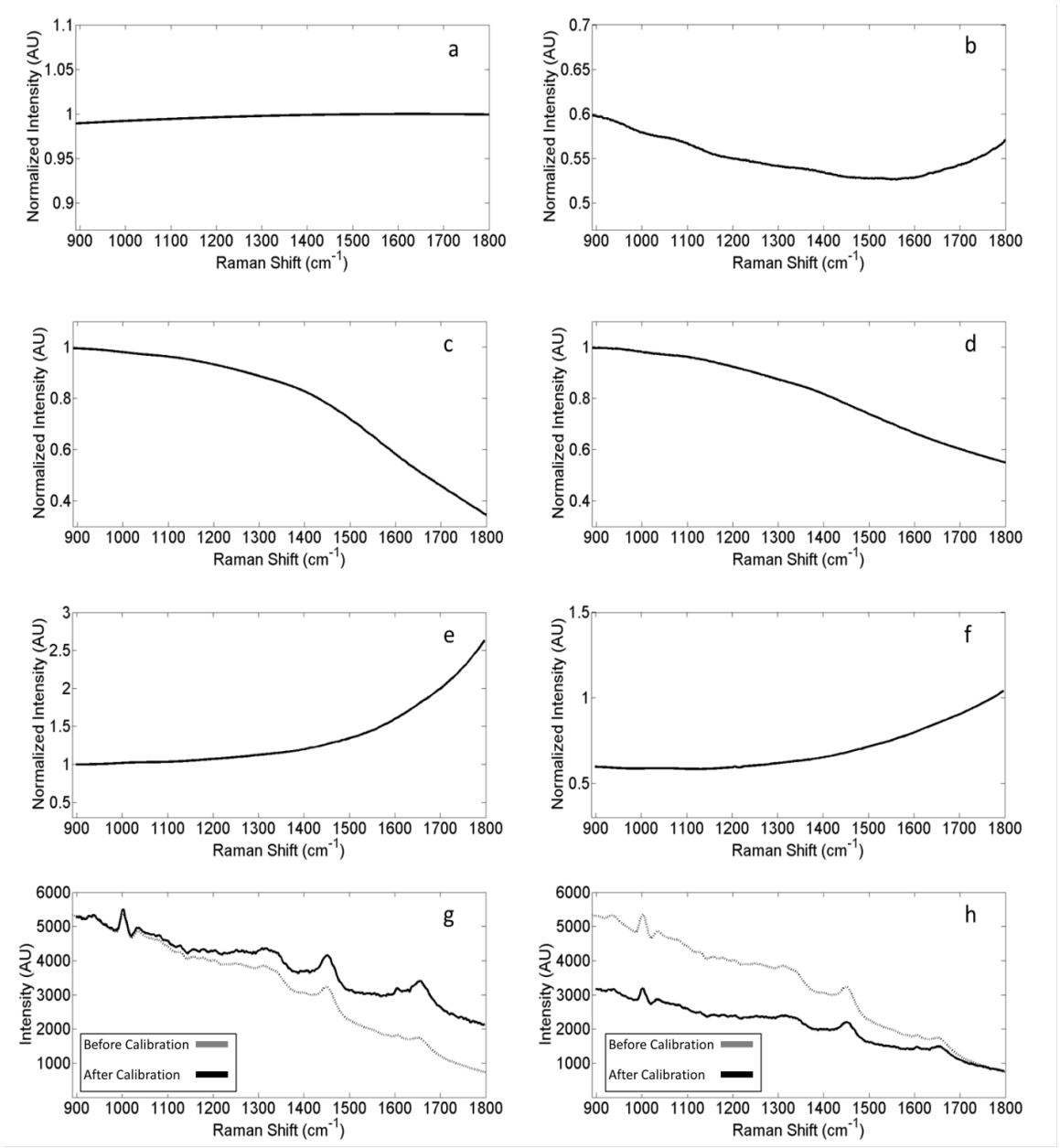


**Figure II.1** (a) Given polynomial for NIST tungsten-lamp. All measured lamp spectra are compared to this curve to obtain the lamp correction factors. (b) Measured glass corrected by NIST tungsten-lamp to obtain the standard for glass correction. All measured glass spectra are compared to this curve to obtain glass correction factors. (c) A spectrum of the tungsten lamp by a fiber-optic probe based system. (d) A spectrum of the glass acquired by a fiber-optic probe based system. (e) Correction factors obtained for the lamp correction method. These factors were determined by dividing the measured curve in (c) to the standard curve in (a). (f) Correction factors obtained by glass calibration. Values were found from dividing the measured glass spectrum (d) into the standard glass spectra (b). (g) The spectrum before lamp correction factors is drawn as a gray line. The spectrum after the lamp correction factors were applied is drawn in black. (h) For the same spectrum as the displayed in (g), the spectrum after glass correction factors are applied is drawn in black and before drawn in gray.

## PROPOSED METHOD

### Glass Determination

The inadequacy of the NIST glass standard leaves the diagnostic Raman community without a method to correct for day-to-day system variations. Each time a system is moved or re-aligned, the response will be altered and must be calibrated. The necessary spectral characteristics of an acceptable standard include a smooth fluorescent curve with little to no Raman signal, no extraneous peaks, throughput across the Raman shift range, and invariance in time and space. Multiple materials were considered to fill this requirement such as plastics, filters, lenses, and different glasses.

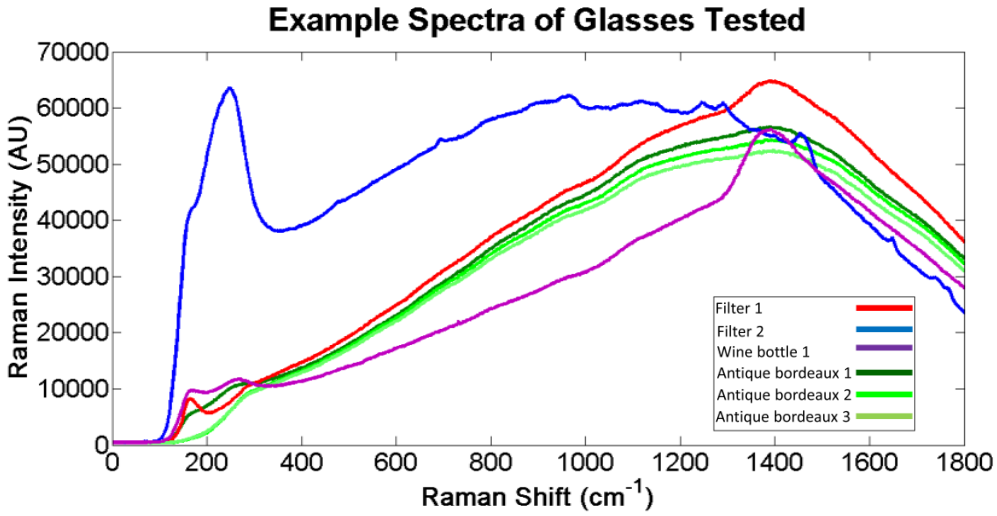


**Figure II.2** Six examples of filters and glasses are displayed above. Filter 1 and Wine bottle 1 both have an extraneous peak at 1400 $cm^{-1}$, making them poor choices as a standard. Filter 2 has Raman signal that does not allow its spectrum to be acceptable. The three glass pieces from different wine bottles colored Antique bordeaux all display a smooth fluorescent curve with no Raman signal or extraneous peaks.

The optimal material found to exhibit the desired characteristics is glass from wine bottles colored “Antique Green Bordeaux”, as shown in Figure II.2. The glass was shown to be temporally and spatially stable, as shown in Figure II.3. Temporal measurements were taken over a 48 hour period, as shown in Figure II.3a, while spatial variability measurements were taken across a sample of size roughly one inch by one inch, displayed in Figure II.3b.

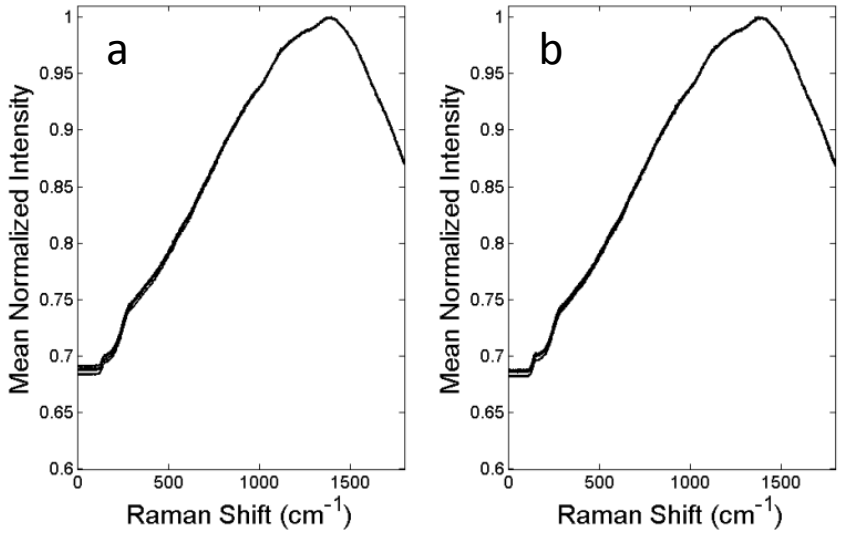


**Figure II.3** (a) Spectra of 5 measurements acquired from different locations in a 1in square of the glass. A lack of spatial variation is displayed by the alignment of all the spectra. (b) Spectra of 5 measurements taken over a time period of 48 hours. A lack of temporal variability is displayed by the alignment of all five curves on top of each other.

**Glass Standard**

The use of glass as a standard makes it possible to correct for small variations within a system on a day-to-day basis. To obtain the ideal glass spectrum for which

comparisons can be made, a spectrum of the glass with a fiber-optic probe based system is acquired. The spectrum is then corrected using the NIST tungsten lamp to obtain the true glass spectrum without being colvolved with the system response curves. This curve is displayed in Figure II.1b. Since the curve is experimentally acquired, it is not smooth like the NIST curve in Figure II.1a. Correction factors determined by the glass spectra are obtained similarly to those of the NIST lamp. For a given system and its alignment, a spectrum of the glass is acquired using the source. This spectrum therefore accounts for changes in system response due to not only the detection leg of a system, but also the source arm. An example of a measured curve is shown in Figure II.1d. Correction factors are then found by dividing the ideal glass spectrum by the measured glass spectrum, as shown in Figure II.1f. These correction factors are then applied to spectra taken with the system. This is shown in Figure II.1h where the gray line is the spectrum before correction and the black line is the calibrated spectrum.

The goal of this study is to determine the viability of antique bordeaux colored glass as a calibration standard for day-to-day system variation. The advantage of this method is to correct for changes in system response using only a single additional spectrum. To validate this method, Raman spectra from three samples were measured while varying components within the system. This includes exchanging the probe for a given spectrometer and exchanging the spectrometer for a given probe.

## Testing and Validation

### Measurement Systems

All spectra were recorded using a fiber-optic probe based Raman spectroscopic system. The source, a M-type laser by (Innovative Photonic Solutions, (Monmouth Junction, NJ) was delivered to the samples by a 400-µm-core-diameter fused-silica optical fiber. This fiber is contained in a fiber-optic probe (EMVision, FL) and surrounded by seven 300- µm fused-silica collection fibers. In-line filters are placed on the delivery and collection fibers to reject signals from the fiber within the generated spectra. The two individual probes chosen for this study both contain this fiber design and except for manufacturing differences, are comparable. Collection fibers are aligned linearly and imaged into a 100 µm entrance slit of the detection system. The detection system is comprised of an imaging spectrograph HoloSpec ƒ/1.8 (Kaiser Optical Systems Inc, MI) and a deep-depletion, back-illuminated, charge-coupled of either model 7534-003 (Acton/Princeton Instruments, NJ) with the chip 256BR. Both imaging spectrographs and CCDs are identical models. The detection system yields a spectral resolution of 7 $cm^{-1}$.

Wavelength calibration of all spectra was executed with a neon-argon lamp. Acetaminophen and naphthalene spectra were used to determine the Raman shift values. All spectra were binned at half the system resolution (3.5 $cm^{-1}$). Spectra were processed and corrected by the NIST calibrated tungsten-light method and glass method. Fluorescence subtraction was performed by a modified polyfit method (Lieber and Mahadevan-Jansen 2003).

All processing was executed by in-house programs written in Matlab (The Mathworks Inc., MA).

**Samples**

Three samples are used to evaluate the potential of glass as a calibration standard. These include acetaminophen, tyrosine, and human cheek skin. Each sample is selected to represent different Raman spectral characteristics. Raman spectra of each sample were from the same localized area of each sample. Acetaminophen and tyrosine samples are assumed homogenous. Acetaminophen was chosen for its low full-width half-maximum and low variability within a sample. Tyrosine samples display a higher fluorescence background and a higher full-width half-maximum than acetaminophen. Last, human skin samples from a cheek were measured *in vivo*. These spectra have the most variability as measurements are taken in the same area, but not perfectly localized. Additionally, skin has a high fluorescence background signal and the highest full-width half-maximum of all three samples. Considering a broad range of samples is necessary to show the broad applicability of the correction method.

**Probe Variation**

While maintaining the laser and spectrometer, two different fiber-optic probes are used to measure spectra from the three samples. Each time a fiber-optic probe is removed, the system response is modified. Therefore, it is important that a calibration method be able to correct for probe changes. Measurements taken from the same sample should only differ due to random noise characteristic of a single system. To reduce this variation, thirty measurements were taken with each probe. Variation between the two systems can therefore be isolated to probe difference and alignment variation.

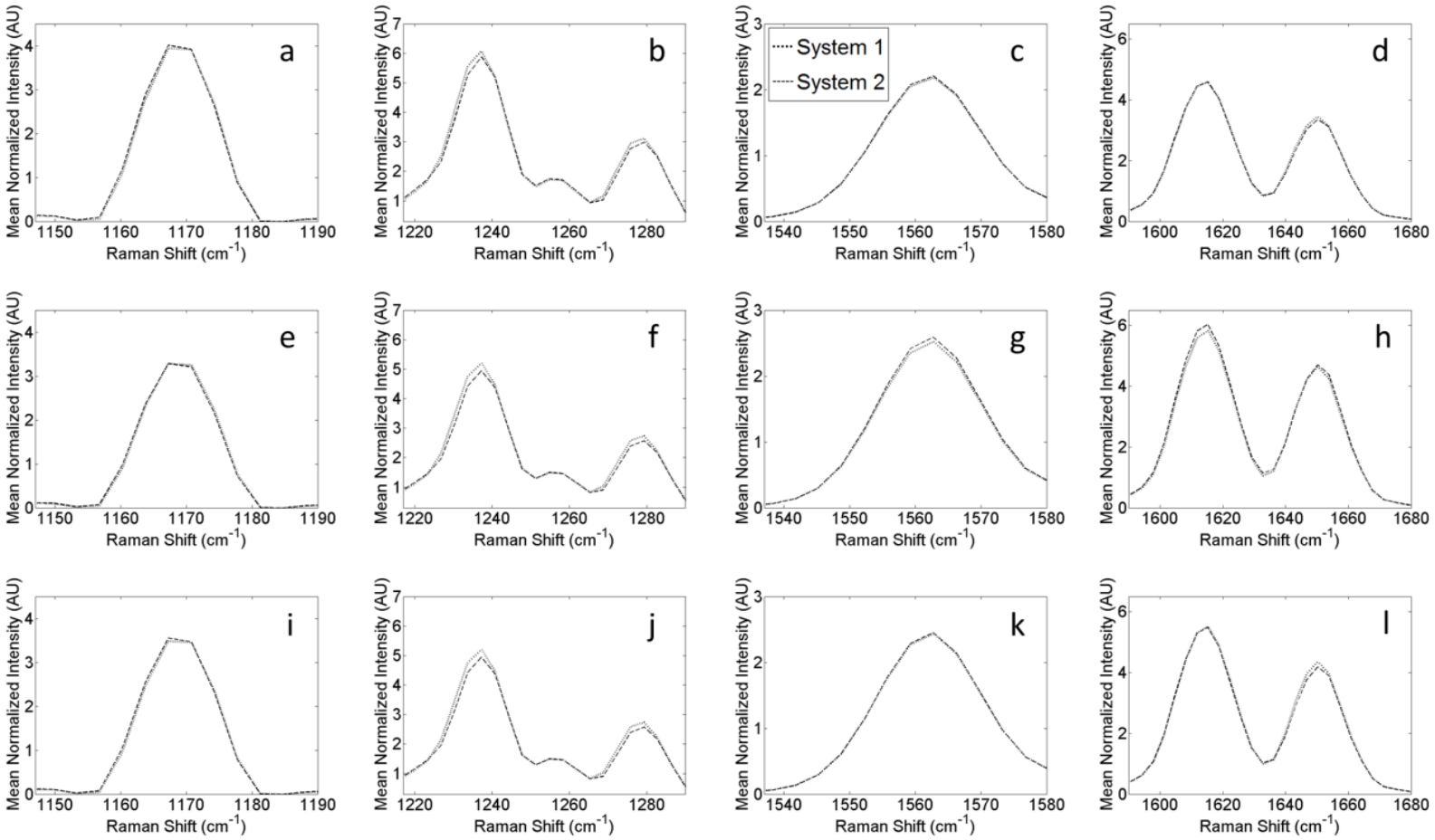


**Figure II.4** Major peaks from acetaminophen spectra. (a, b, c, d) Non-corrected spectra, (e, f, g, h) lamp corrected spectra, (i, j, k, l) and glass corrected spectra. From left to right, spectral peaks are shown by increasing Raman shift. Both glass and lamp calibration methods indicate the ability to remove intensity differences at some peaks. A limitation of both calibration methods is seen by the spectra when two peaks are connected by both methods only correcting for one peak and not the other.

The spectrum for acetaminophen is known for low, stable peaks as it is often used in calibrating wavelengths. Without large amounts of variation in its spectrum, changes in a system's response are difficult to detect visually. Figure II.4 displays selected peaks of interest for acetaminophen spectra. The peaks at 1170 $cm^{-1}$ do not differ among non-corrected, lamp corrected, and glass corrected spectra. Neither correction method affects spectral regions where there is no difference between the two spectra from each probe. At 1560 $cm^{-1}$ however, calibration by the lamp caused a difference between the spectra from both probes where there was none initially. A limitation of both correction methods is illustrated by the peaks at 1610 $cm^{-1}$ and 1650 $cm^{-1}$, which are overlapping. Without correction, there is only a difference between the two spectra at 1650 $cm^{-1}$. The lamp correction method fixes this difference, at 1650 $cm^{-1}$, at the expense of the 1610 $cm^{-1}$ peak. Glass correction does not alter the intensity differences at 1650 $cm^{-1}$, but does not alter the 1610 $cm^{-1}$ peak. The last peaks of interest, at 1230 $cm^{-1}$ and 1280 $cm^{-1}$, are also without a complete valley between them. No large differences are seen between the spectra from both probes for uncorrected, lamp corrected, or glass corrected data. Unlike the 1610 $cm^{-1}$ and 1650 $cm^{-1}$ peaks, these peaks are not altered by either method. Both methods of calibration have shown the ability to decrease differences in peak intensity due to probe variation.

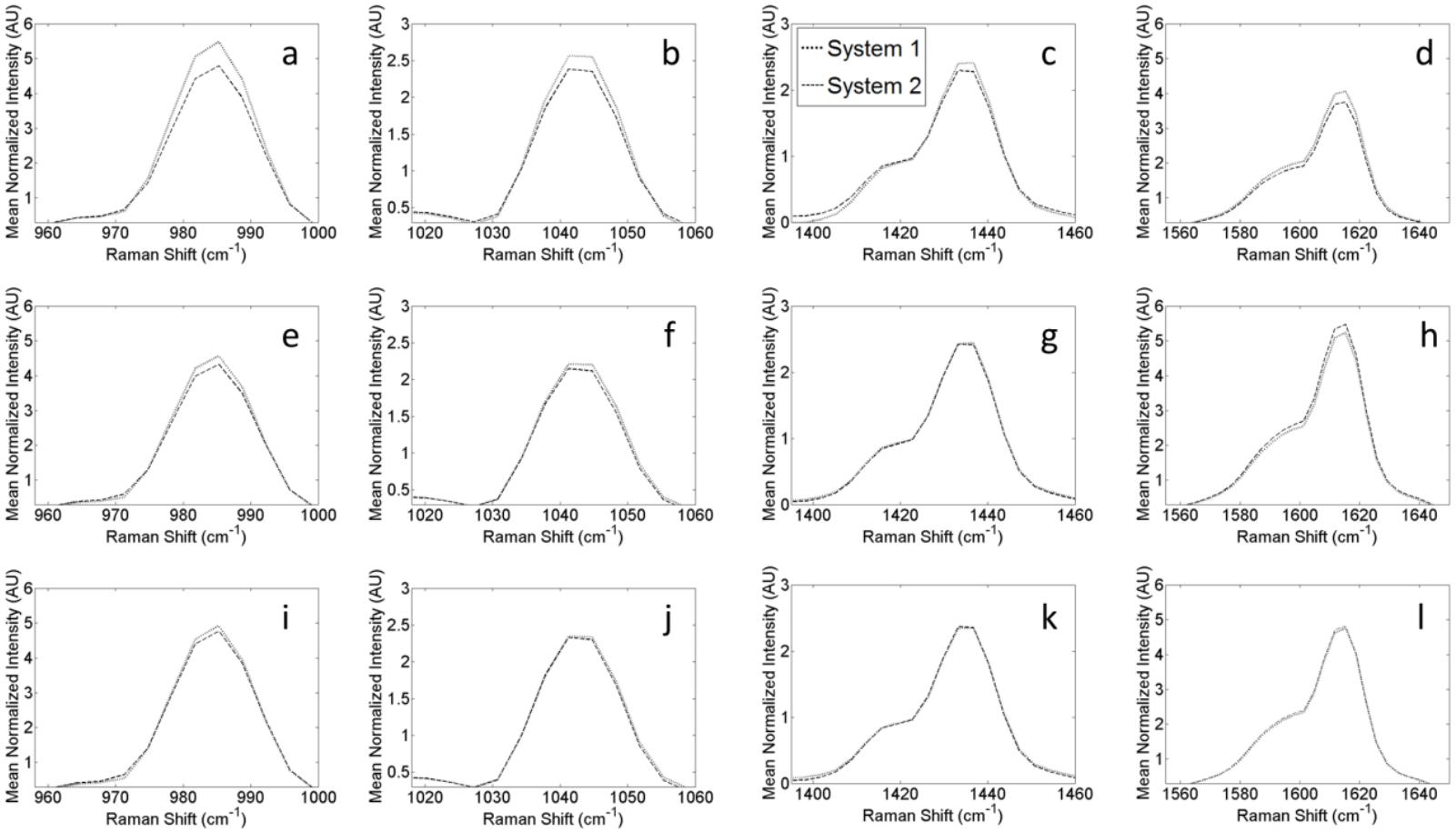


**Figure II.5** Major peaks from tyrosine spectra. (a, b, c, d) Non-corrected spectra, (e, f, g, h) lamp corrected spectra, (i, j, k, l) and glass corrected spectra. From left to right, spectral peaks are shown by increasing Raman shift. Glass and lamp calibration methods demonstrate their ability to decrease peak differences due to system throughput response changes from varying the probe.

Though small, the spectra from varying probes on tyrosine samples show statistically significant difference. There is an observable difference in peak intensity at 985 $cm^{-1}$, 1040 $cm^{-1}$ and 1615 $cm^{-1}$. Calibration of the spectra by the lamp at each peak reduces the differences in intensity, however does not fully eliminate all separation. The glass correction is able to further reduce (Figure II.5i) or eliminate (Figures II.5j and II.5l) the intensity differences between spectra. Peaks that are fully corrected by the lamp calibration method are also fully corrected by the glass calibration method (Figures II.5g and II.5k). These examples illustrate the potential of both methods to correct for subtle differences in intensity due to variation in system throughput.

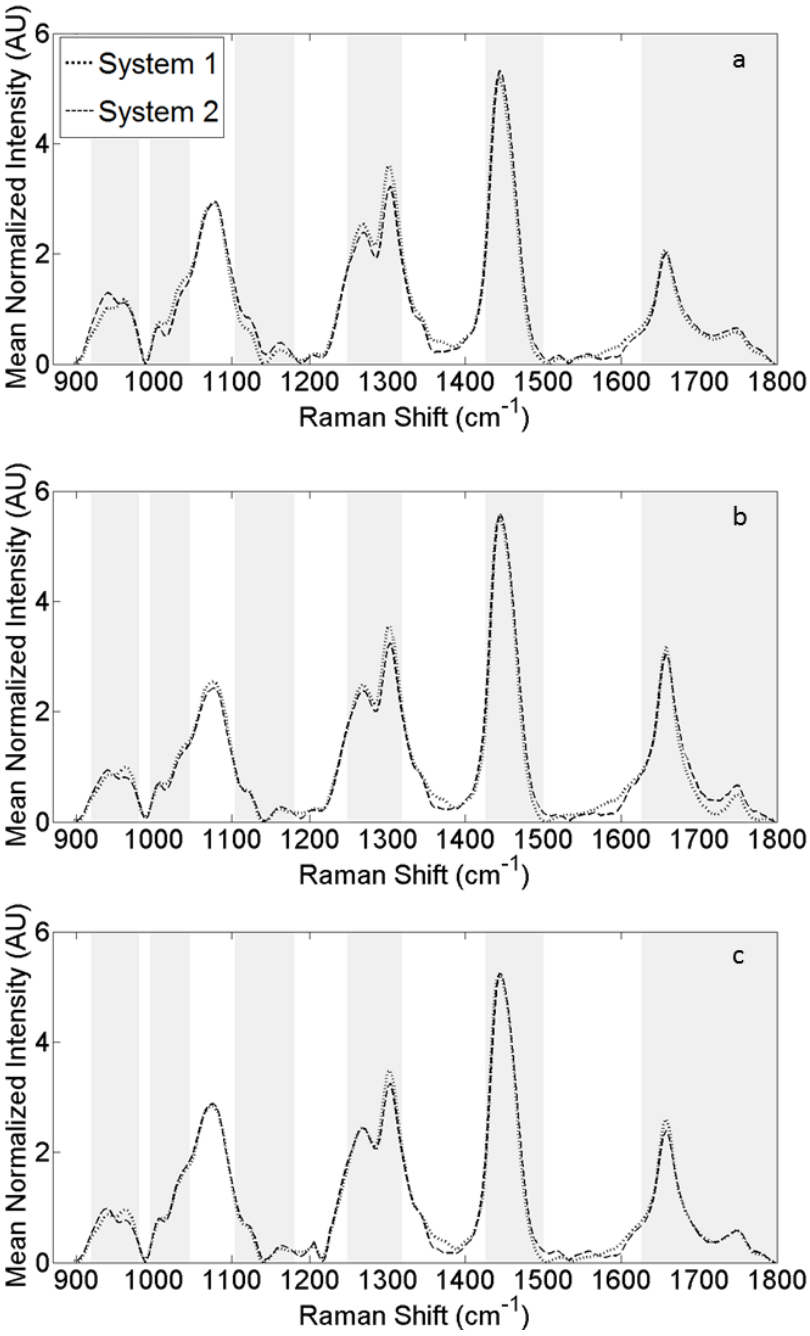


**Figure II.6** (a) Cheek skin spectra not corrected, (b) lamp corrected, (c) and glass corrected. Both glass and lamp calibration methods are able to decrease intensity differences in the spectral peaks. A limitation to both methods is the conjoining of peaks where each method increases spectral difference at one location when elsewhere.

As a final verification of this method, human cheek samples are used to judge applicability of these correction methods for spectra with wide peaks and high fluorescence. Gray shaded areas, in Figure II.6, indicate selected areas of difference in spectra between non-corrected, lamp corrected, and glass corrected data. It can be seen that there are many places where both, lamp and glass correction methods are able to correct for intensity differences between the two spectra. Some of these points include peaks and shoulders at 1010 $cm^{-1}$, 1110 $cm^{-1}$, 1280 $cm^{-1}$, 1300 $cm^{-1}$, and 1450 $cm^{-1}$. Generally, the glass calibration method reduces spectral differences more effectively for probe variation. The one instance where this is not observed is within the region of the peaks at 1650 $cm^{-1}$ to 1750 $cm^{-1}$. At this location, the glass method introduces a greater degree of difference at the 1650 $cm^{-1}$ peak to correct for a significant difference in the valley and 1750 $cm^{-1}$ peak. The lamp calibration method introduces less intensity differences at the 1650 $cm^{-1}$ peak, but causes great variation in the adjacent valley and 1750 $cm^{-1}$ peak. It can be seen from the full spectra that both glass and lamp calibration methods decrease intensity differences.

The spectra from acetaminophen, tyrosine, and human cheek display the potential of glass method to correct spectra similar to the tungsten lamp for differences in throughput due to a fiber-optic probe. This is important as a lamp spectrum can be difficult to obtain for daily measurements. The acquisition of a glass spectrum however, only takes the cost of an additional measurement.

**Instrument Variation**

Variation due to the probe must be corrected in fiber-optic probe based systems to reliably use Raman spectroscopy as an analytical tool. However, effects of spectrometer variation are important for broad application of these correction methods. To test the limitations of lamp and glass calibration, a probe connected to two spectrometers measured the three samples. Intensity differences should only occur due to variation in instrument throughput, which are expected to be small.

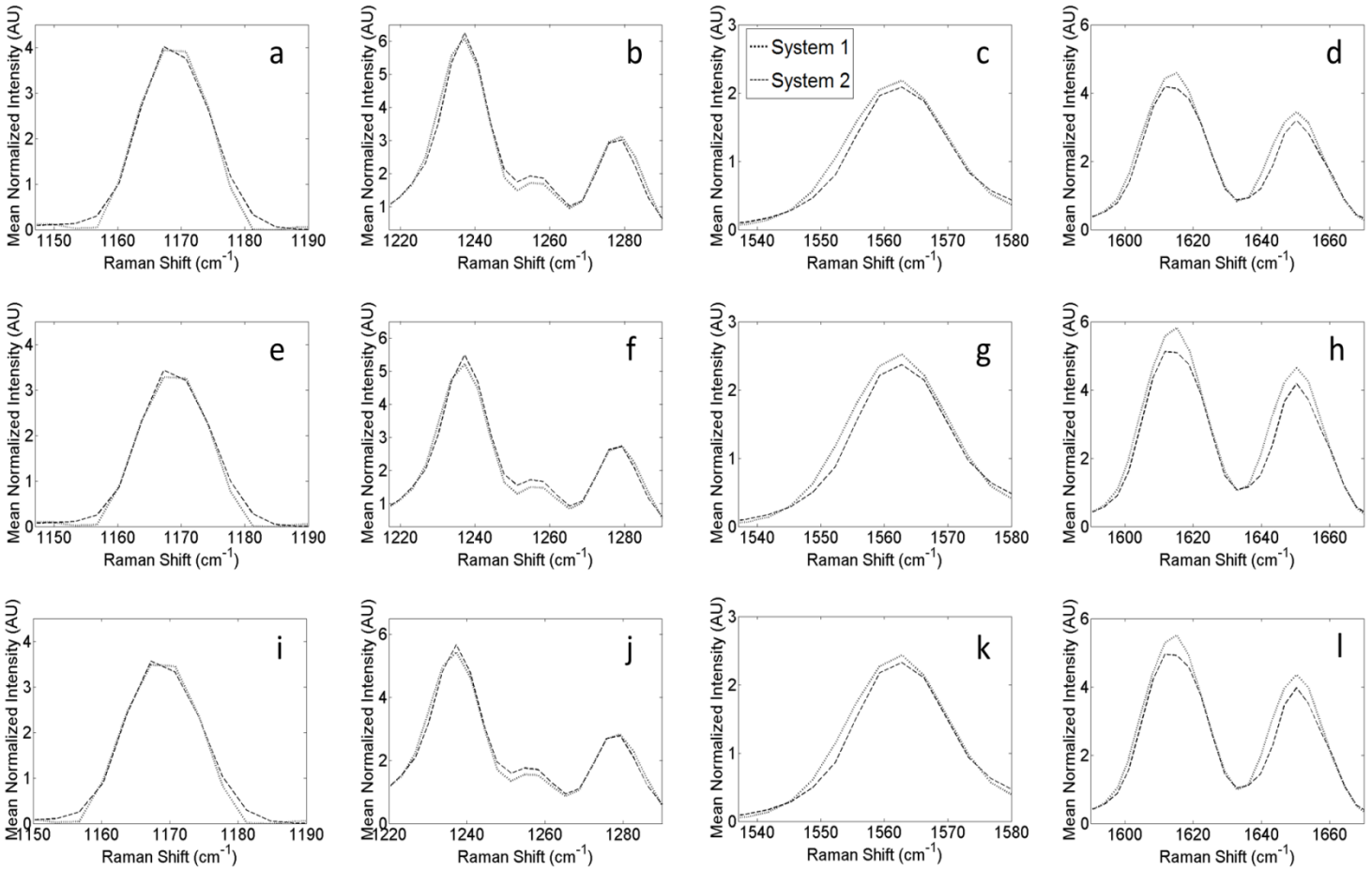


**Figure II.7** Major peaks from acetaminophen spectra. (a, b, c, d) Non-corrected spectra, (e, f, g, h) lamp corrected spectra, (i, j, k, l)and glass corrected spectra. From left to right, spectral peaks are shown by increasing Raman shift. Both calibration methods display their weakness in correcting for small spectral intensity differences due to spectrometer variation.

Spectral peaks for acetaminophen due to changes in spectrometers are shown in Figure II.7. The acetaminophen sample showed both correction methods do not fully correct for intensity variations; however, neither method introduces significant intensity differences. This illustrates the limitation for both calibration methods when correcting spectra of samples with strong peaks and low fluorescence in the case of different spectrometers.

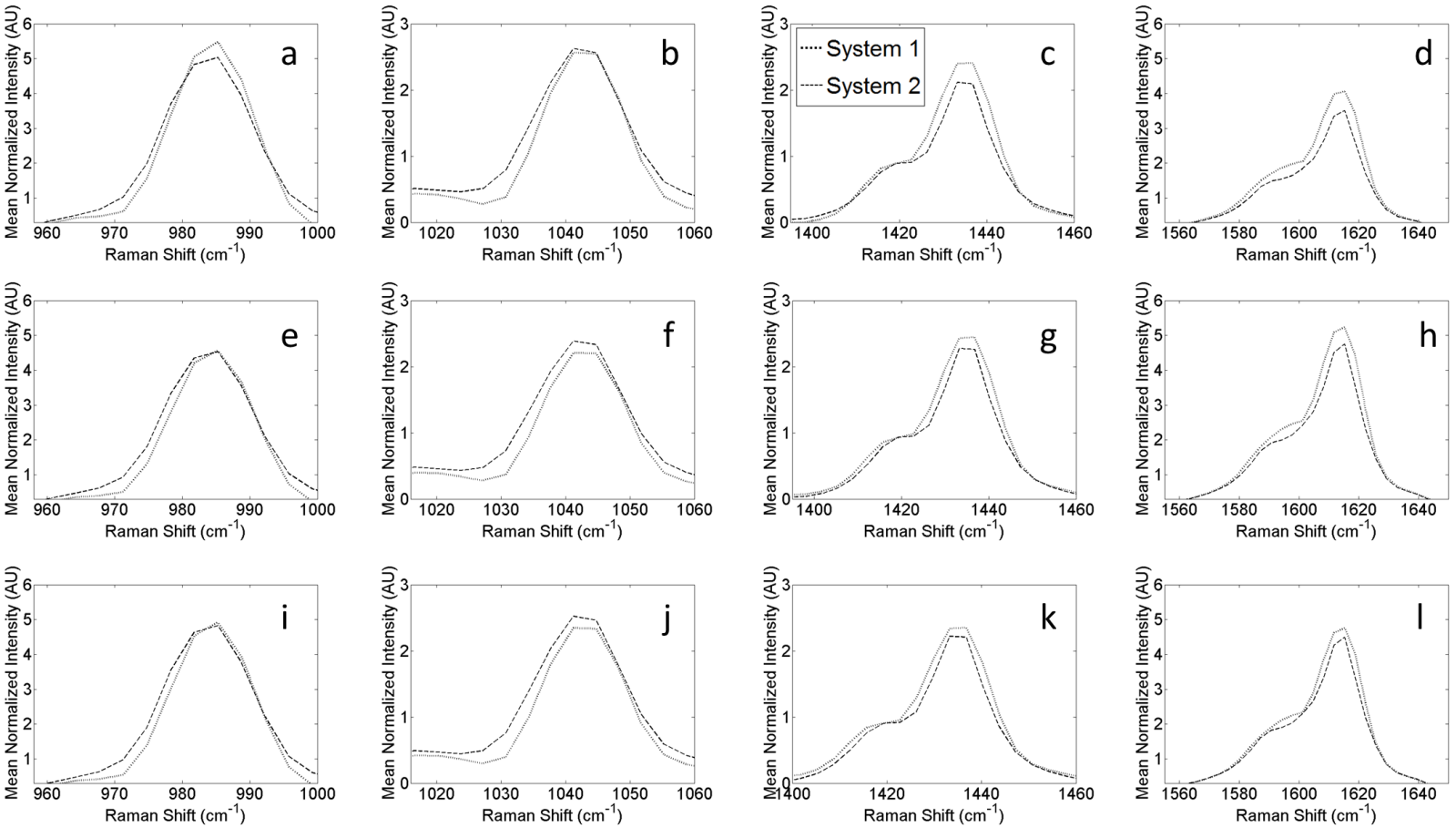


**Figure II.8** Major peaks from tyrosine spectra. (a, b, c, d) Non-corrected spectra, (e, f, g, h) lamp corrected spectra, (i, j, k, l) and glass corrected spectra. From left to right, spectral peaks are shown by increasing Raman shift. Glass and lamp calibration display the ability to correct at specific peaks when the spectrometer is varied for tyrosine spectra. However, both methods also increased the intensity difference between the two spectra at the 1045 $cm^{-1}$ peak.

In contrast, samples of tyrosine (Figure II.8) demonstrate a more significant modification by both methods. At certain peaks, 1045 $cm^{-1}$ for example, a noticeable increase in intensity difference is observed for both calibration methods. However, both methods do correct significantly at other peaks, such as at 985 $cm^{-1}$ and 1435 $cm^{-1}$. Furthermore, isolated cases, such as the peak at 1615 $cm^{-1}$, demonstrates a greater degree of correction by the glass method. The ability to correct for spectrometer variation in some instances is displayed by the tyrosine spectra.

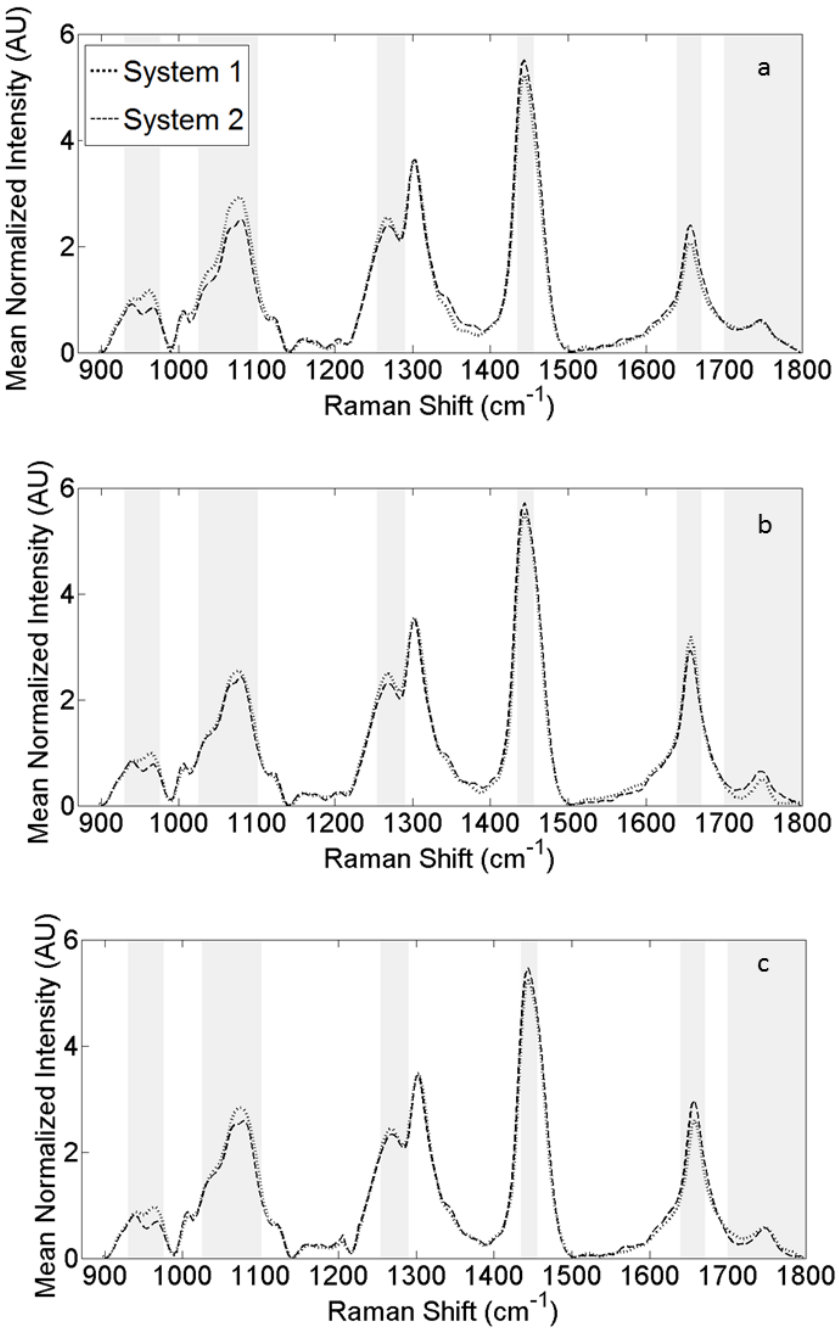


**Figure II.9** (a) Cheek skin spectra not corrected, (b) lamp corrected, and (c) glass corrected. When the spectrometer for skin spectra is altered, both calibration methods illustrated the ability to correct for some intensity differences, but not all locations of variation. As seen above when the probe was varied, both methods had trouble correcting for the 1650 $cm^{-1}$ and 1750 $cm^{-1}$ peaks.

The effect of varying the spectrometer while sampling human cheek skin, shown in Figure II.9, demonstrates both methods correct for intensity differences differently. There are instances where the lamp calibration method corrects better than the glass method, for example 1050 $cm^{-1}$. Conversely, there are peaks where spectra corrected by the glass method display smaller intensity differences than those of the lamp correction. One example of this is the peak at 1280 $cm^{-1}$. Additionally, the peaks at 1650 $cm^{-1}$ and 1750 $cm^{-1}$ are corrected in a similar fashion as they were when the probe was varied. Overall, there seems to be a tradeoff which was not observed in the previous cases.

These three samples collectively illustrate the capabilities of each correction method to reduce intensity differences caused by spectrometer variation. Though not as effective as when correcting for probe variation, the general trend positively corrects for throughput differences.

**Statistical Variance**

To quantify the changes in peaks, box plots were used to display the overall variance ranges for each correction method. Box plots provide a holistic approach to illustrate the deviation between spectra from each system graphically and quantitatively. Most important is the median value and quartiles which represent information from the whole range of Raman shifts. Variance was calculated between the two systems for the measured data (n=60) at each Raman shift. The values for the variance at all Raman shifts were then used to create a boxplot for each method. The shorter and lower median variance value indicates the spectra from each system tested

are closer together ie, the intensity difference in spectra is smaller. Some variance is still expected as no correction method is perfect and noise will always exist in measurements.

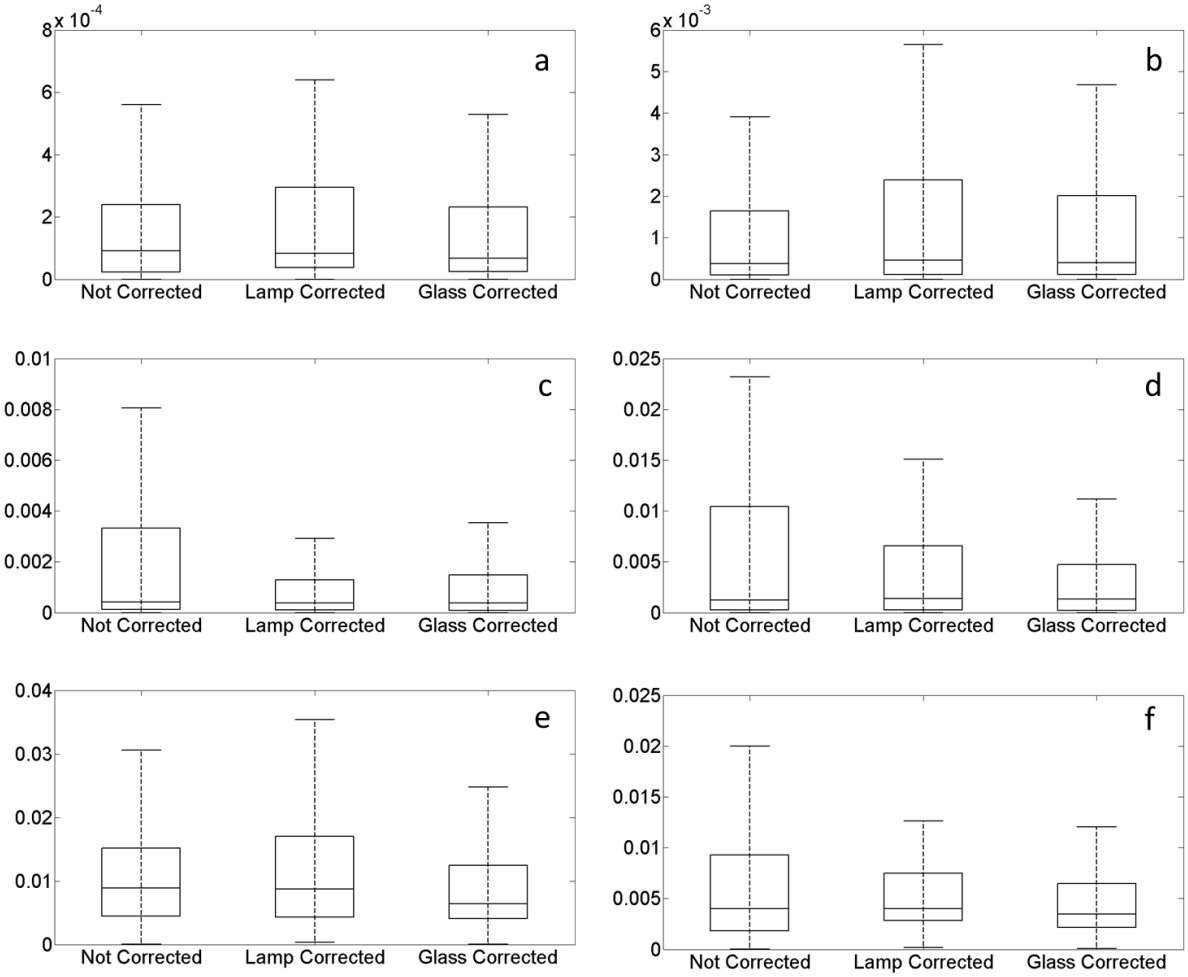


**Figure II.10** Spectral variance between measurements plotted through box plots. (a) Acetaminophen probe variation, (b) acetaminophen instrument variation, (c) tyrosine probe variation, (d) tyrosine instrument variation, (e) cheek skin probe variation, (f) cheek skin instrument variation. A decrease in the median values is displayed for lamp and glass correction when the probe is changed. Glass correction illustrates the ability to additionally decrease the 75$^{th}$ quartile and maximum variance values for the three samples tested whereas the lamp correction method does not. For the variation in spectrometers, both lamp and glass correction have the same median variance value as the un-corrected data. However, the glass and lamp correction method decrease the maximum and 75$^{th}$ quartile variance values from the un-corrected data.

The results of this analysis are displayed in Figure II.10. Lamp and glass correction methods both display a decrease in overall variance as the probe is varied for measurements on acetaminophen and tyrosine. The skin spectra do not display a decrease in variance for both methods. Variance is only decreased by the glass calibration method and not the lamp method. These results indicate that glass calibration can more accurately correct for day-to-day variation caused by a probe. When the spectrometer is varied, the median variance shows no change for either correction method in the three samples. For tyrosine and skin spectra, where there is a greater initial variance in measurements, both calibration methods reduce the range of variances. Furthermore, the reduction by the glass correction method is greater than that of the lamp. For example, Figure II.10d displays a reduction in the $75^{th}$ quartile and maximum variance for lamp correction. Additionally, the glass calibration method shows an even further reduction in the $75^{th}$ quartile and maximum variance values. This indicates that both methods are reducing variance caused by different spectrometers, though the glass method indicates a higher effectiveness.

This analysis quantifies and verifies the general trend observed in the processed spectra illustrating the proficiency of the glass correction method. A reduction in variance for all samples in both probe variation and spectrometer variation displays the potential impact glass correction can have on changes to the system response.

**Conclusion**

The ability to correct for changes in the system response is necessary to accurately classify substances or differences between samples. Day-to-day variations introduces significant differences in spectral intensities which must be corrected for. System response variation can be caused by slight movements of optics and the removal and reattachment of the fiber-optic probe. The method presented here can be easily performed in all measurement situations, including medical environments. Furthermore, the standard, antique bordeaux colored glass, is easily portable and inexpensive. The data presented displays the capabilities and limitations of both correction methods, the lamp and glass. However, for probe and spectrometer variation, a greater decrease between spectra is shown when the glass method is used to correct. As Raman spectroscopy is further integrated into diagnostic medical applications, the use of a calibration method like the glass will become increasingly important.

## Bibliography


Choquette, S. (2005). "Standard reference materials for relative intensity correction of Raman spectrometers." American Laboratory **37**(22): 22-+.

Choquette, S. J., E. S. Etz, et al. (2007). "Relative intensity correction of Raman spectrometers: NIST SRMs 2241 through 2243 for 785 nm, 532 nm, and 488 nm/514.5 nm excitation." Applied Spectroscopy **61**(2): 117-129.

DeRose, P. C., E. A. Early, et al. (2007). "Qualification of a fluorescence spectrometer for measuring true fluorescence spectra." Review of Scientific Instruments **78**(3).

DeRose, P. C., E. A. Early, et al. (2008). Measuring and Certifying True Fluorescence Spectra with a Qualified Fluorescence Spectrometer. 5th Oxford Conference on Spectrometer, Crown, UK.

DeRose, P. C., M. V. Smith, et al. (2008). "Characterizaton of Standard Reference Materials 2941, Uranyl-Ion-Doped Glass, Spectral Correction Standard for Fluorescence." Journal of Luminescence **128**: 257-266.

DeRose, P. C., M. V. Smith, et al. (2009). "Characterization of Standard Reference Materials 2940, MN-Ion-Doped Glass, Spectral Correction Standard for Fluorescence." Journal of Luminescence **129**: 349-355.

Frost, K. J. and R. L. McCreery (1998). "Calibration of Raman spectrometer instrument response function with luminescence standards: An update." Applied Spectroscopy **52**(12): 1614-1618.

Keller, M. D., E. M. Kanter, et al. (2008). "Detecting temporal and spatial effects of epithelial cancers with Raman spectroscopy." Disease Markers **25**(6): 323-337.

Keller, M. D., E. M. Kanter, et al. (2006). "Raman spectroscopy for cancer diagnosis." Spectroscopy **21**(11): 33-41.

Lackowicz, J. R. (1999). Principles of Fluorescence Spectroscopy. New York, Kluwer Academic/Plenum Publishers.

Lieber, C. A. and A. Mahadevan-Jansen (2003). "Automated method for subtraction of fluorescence from biological Raman spectra." Applied Spectroscopy **57**(11): 1363-1367.

Lieber, C. A., S. K. Majumder, et al. (2008). "Raman microspectroscopy for skin cancer detection in vitro." Journal of Biomedical Optics **13**(2).

Locascio, L. and R. Watters (2010). Standard Reference Material 2241. Relative Intensity Correction Standard for Raman Spectroscopy: 785 nm Excitation. Gaithersburg, MD, National Institute of Standards and Technology; Department of Commerce, United States of America**:** 6.

Mahadevan-Jansen, A. and R. Richards-Kortum (1996). "Raman Spectrscopy for the Detection of Cancers and Precancers." Journal of Biomedical Optics **1**(1): 31-70.

Vo-Dinh, T., L. R. Allain, et al. (2002). "Cancer gene detection using surface-enhanced Raman scattering (SERS)." Journal of Raman Spectroscopy **33**(7): 511-516.

Whisenant, J. and N. Gasparino (2007). Raman Spectroscopy: A Quantitative Assessment of Spectral Variation and Clinical Application. Biomedical Engineering. Nashville, Vanderbilt University. **Master of Engineering:** 49.

# CHAPTER III

# CONCLUSIONS AND FUTURE DIRECTIONS

## Future Applications

This study shows that calibration by glass can correct for changes in system response of Raman spectroscopic systems. Therefore, a new standard for fiber-optic probe based systems is now available. As system variance is always present due to small system movements, probe reattachment, and slit and lens adjustments, correction must be implemented constantly in Raman spectroscopy systems so that data is accurate. Glass correction is especially helpful in situations where taking measurements of the NIST Tungsten-lamp is not feasible, for example in biomedical Raman spectroscopy studies.

### Clinical Applications

Raman spectroscopy has shown to be a viable method of detecting diseased versus healthy tissue for many illnesses, including cancer (Mahadevan-Jansen, Mitchell et al. 1998; Gebhart, Lin et al. 2006; Kanter, Majumder et al. 2009; Bi, Walsh et al. 2010; Patil, Krishnamoorthi et al. 2010). The technique is able to distinguish small biochemical changes in tissue which result from pathological differences. The changes in healthy tissue are often small and difficult to distinguish; therefore, statistical classification algorithms are used to classify a measured sample. If the differences in spectra due to

the system variation are as large as those due to tissue differences, Raman spectroscopy results will be inaccurate and thus useless for diagnosis. Due to patient care, NIST tungsten-lamp correction is difficult to use as a correction source. Glass correction, based on the measurement of an antique bordeaux colored glass, can be done in clinical environments. The Raman spectra of skin greatly varies between patients due to pigmentation and texture differences as well as due to chemical makeup. This variability can cause difficulty in distinguishing diseased skin from healthy skin. The use of multiple systems to acquire data only increases spectra differences more (Pence, Patil et al. 2011). Figure III.1 displays a preliminary result found from a skin cancer study. All four measurements are from four unique systems on four separate individuals who all have healthy tissues. With no correction for system variation, all four spectra are vastly different from each other, indicating the difficulty to classify all spectra the same way. The lamp calibration method displays an ability to correct for some instances of difference, but does not resolve the problem. However, glass calibration significantly reduces variations so that all the healthy patients can be distinguished equal. The variation left is likely due to filter differences and inherent patient and measurement site differences. Different types of filters will cause light to be blocked differently. As both correction methods are based on collected light, neither correction method can correct perfectly for light in this region as it is not detected for. Additionally, inherent patient differences will always occur in spectra as measurements are based on chemical differences and the biochemical differences of individuals are not what the system correction methods are meant to correct for. This preliminary study towards applying

glass correction to clinical situations is promising for its ability to correct for spectral differences. Future work should include glass calibration towards a wider patient data set and other clinical studies.

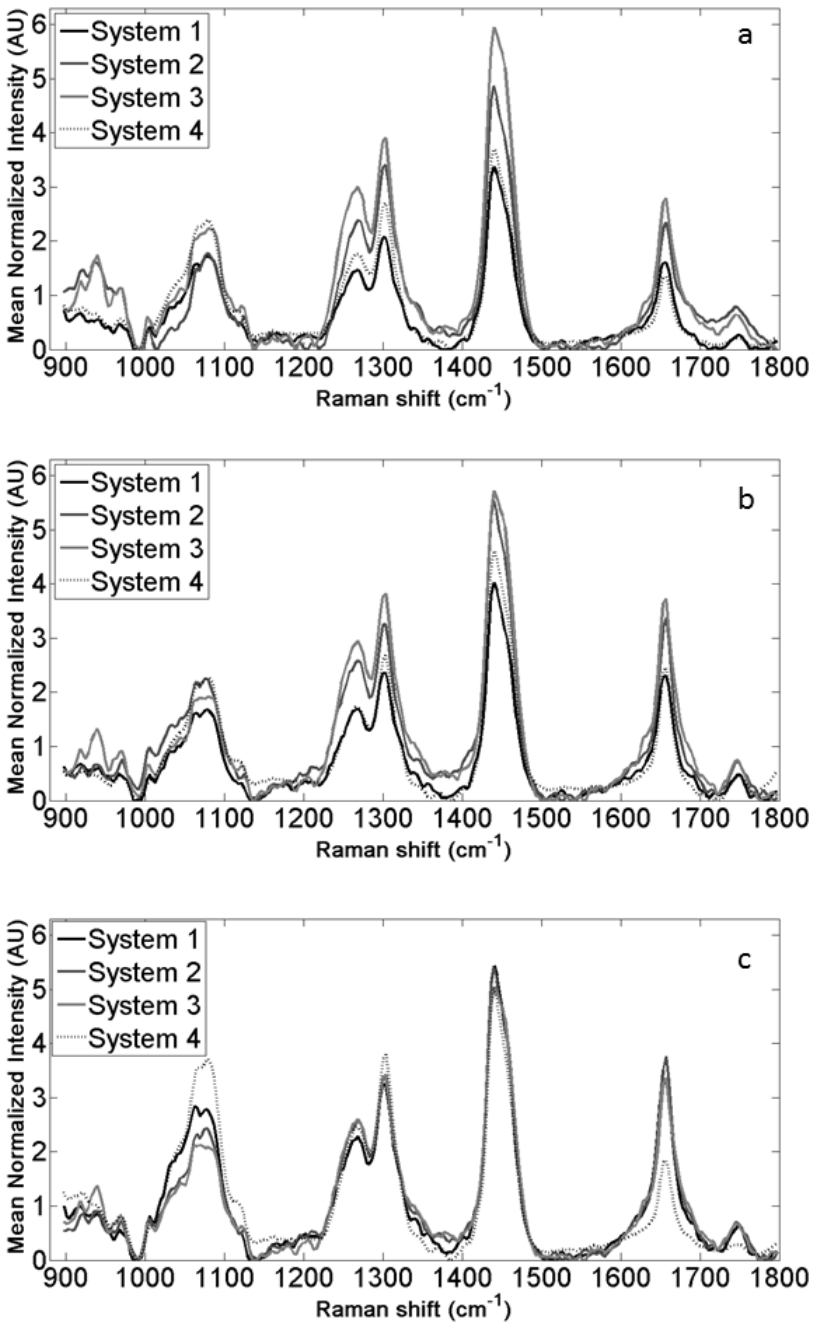


**Figure III.1** Spectra of healthy skin from four healthy patients. Spectra are un-corrected (a), lamp corrected (b), and glass corrected (c). A decrease in spectral intensity can be viewed for the lamp correction method. However, a further decrease in spectral intensity is illustrated by the glass calibration method. Glass calibration causes main peaks to align, greatly reducing the overall variation between the spectra. The variability in the four spectra left is due to patient and measurement location variability.

**Non Fiber-optic Probe Based Raman Spectroscopy Systems**

The results from this study are based on fiber-optic probe based Raman spectroscopy systems. There are many unique Raman spectroscopy systems commercially available and many more home-built systems. All of these systems will have day-to-day variation, due to the slight movement of components. Glass calibration is a potential method to correct for system response changes in different types of Raman spectroscopic instruments regardless of the type of instrument. A combined Raman-spectroscopy and Optical Coherence Tomography system has been built in our lab (Patil, Bosschaart et al. 2008; Patil, Krishnamoorthi et al. 2010; Patil, Kirshnamoorthi et al. 2011). This system has been using a piece of Antique Bordeaux glass as a method to correct for its day-to-day variation with promising results for the last few months. Further studies on the ability of calibration by glass to correct for system throughput changes will be studied in the future.

## Conclusions

A new method to correct for system variation due to probe differences has been developed. This method has been validated through the testing of three unique samples including, acetaminophen, tyrosine, and cheek skin *in vivo*. The use of this new correction method will help researchers correct for variation between multiple probes and data variation due to the removal and reattachment of a fiber-optic probe. The standard for correction, antique bordeaux colored glass, is inexpensive and easily obtained. Additionally, the spectrum can be measured in clinical situations, allowing

researchers using Raman spectroscopy of a diagnostic tool to benefit from the correction method.

## Bibliography


Bi, X., A. Walsh, et al. (2010). "Using Raman Spectroscopy to Discriminate Inflammatory Bowel Diseases." Diseases of the Colon & Rectum **53**(4): 540-541.

Gebhart, S. C., W. C. Lin, et al. (2006). "In vitro determination of normal and neoplastic human brain tissue optical properties using inverse adding-doubling." Physics in Medicine and Biology **51**(8): 2011-2027.

Kanter, E. M., S. Majumder, et al. (2009). "Effect of hormonal variation on Raman spectra for cervical disease detection." American Journal of Obstetrics and Gynecology **200**(5): -.

Mahadevan-Jansen, A., M. F. Mitchell, et al. (1998). "Near-infrared Raman spectroscopy for in vitro detection of cervical precancers." Photochemistry and Photobiology **68**(1): 123-132.

Patil, C., H. Krishnamoorthi, et al. (2010). "Combined Raman Spectroscopy-Optical Coherence Tomography for the Detection of Skin Cancers." Lasers in Surgery and Medicine: 16-17.

Patil, C. A., N. Bosschaart, et al. (2008). "Combined Raman spectroscopy and optical coherence tomography device for tissue characterization." Optics Letters **33**(10): 1135-1137.

Patil, C. A., H. Kirshnamoorthi, et al. (2011). "A Clinical Instrument for Combined Raman Spectroscopy-Optical Coherence Tomography of Skin Cancers." Lasers in Surgery and Medicine **43**(2): 143-151.

Pence, I. J., C. A. Patil, et al. (2011). Characterizing variability in Raman Spectra of benign lesions toward cancer detection in skin. SPIE Photonics West Photonics in Dermatology and Plastic Surgery, San Francisco, CA.